VALIDATION OF IMAGE BASED THERMAL SENSING TECHNOLOGY FOR GLYPHOSATE RESISTANT WEED IDENTIFICATION

A Thesis
Submitted to the Graduate Faculty
of the
North Dakota State University
of Agriculture and Applied Science

By

Austin Joshua Eide

In Partial Fulfillment of the Requirements
for the Degree of
MASTER OF SCIENCE

Major Program:
Natural Resource Management

November 2020

Fargo, North Dakota

North Dakota State University
Graduate School

Title

VALIDATION OF IMAGE BASED THERMAL SENSING TECHNOLOGY FOR GLYPHOSATE RESISTANT WEED IDENTIFICATION

By

Austin Joshua Eide

The Supervisory Committee certifies that this ***disquisition*** complies with North Dakota State University's regulations and meets the accepted standards for the degree of

MASTER OF SCIENCE

SUPERVISORY COMMITTEE:

Xin Sun
Chair

Yu Zhang

Joao Paulo Flores

Jack Norland

Approved:

November 19, 2020
Date

Edward DeKeyser
Department Chair

ABSTRACT

From 2019 to 2020, greenhouse and field research was conducted at North Dakota State University to investigate the canopy temperature response of waterhemp (*Amaranthus rudis*), kochia (*Kochia scoparia*), common ragweed (*Ambrosia artemisiifolia*), horseweed (*Conyza canadensis*), Palmer amaranth (*Amaranthus palmeri*), and red root pigweed (*Amaranthus retroflexus*) after glyphosate application to identify glyphosate resistance. In these experiments, thermal images were captured of randomized glyphosate resistant populations and glyphosate susceptible populations of each weed species. The weed canopies' thermal values were extracted and submitted to statistical testing and various classifiers in an attempt to discriminate between resistant and susceptible populations. Glyphosate resistant horseweed, when collected within greenhouse conditions, was the only biotype reliably classified using significantly cooler temperature signatures than its susceptible counterpart. For field conditions, image based machine learning classifiers using thermal data were outperformed by classifiers made using additional multispectral data, suggesting thermal is not a reliable predictor of glyphosate resistance.

ACKNOWLEDGMENTS

I would like to extend my sincerest gratitude to my academic and thesis advisor Dr. Xin Sun for accepting me as part of his research group and for encouraging me to pursue higher endeavors. I would also like to extend thanks to my advisory committee: Drs. Joao Paulo Flores, Yu Zhang, and Jack Norland. A special thanks goes to Dr. John Stenger, whose patience and conveyance of wisdom made me a better agriculturalist, worker, and person. Additionally, I would like to thank Dr. Kirk Howatt, Sandy Johnson, and Joseph Mettler for their use of resources, their assistance in field work, and for supplying weed populations for my study. Finally, I would like to thank John Nowatzki, whose guidance fostered a strong passion for precision agriculture throughout my undergraduate years.

TABLE OF CONTENTS

LIST OF TABLES

LIST OF FIGURES

1. INTRODUCTION

1.1. Purpose of Study

In the spring of 2017, researchers at North Dakota State University pursued a method of herbicide resistance detection that utilized thermal imaging technology. The research team hypothesized that glyphosate resistant populations of ragweed, waterhemp, and kochia would have lower canopy temperatures in comparison to susceptible populations immediately after glyphosate application and that the differences could be used to develop a support vector machine (SVM) classifier to identify glyphosate resistant weeds (Shirzadifar, 2018). This study was performed to validate the original method and had the potential to offer valuable insight into the value of thermal data within agriculture. Developing a method that can differentiate and geotag weeds that exhibit herbicide resistance with thermal imagery within an acceptable timeframe after application has great potential to help growers manage their fields more effectively.

1.1.1. Objectives of Study

The goal of this project was to validate the previously developed method to identify herbicide resistance in weeds in true field conditions by integrating thermal and multispectral sensing methods to statistically analyze the thermal response of six weed species to glyphosate application. The species investigated in this study are waterhemp (*Amaranthus rudis*), kochia (*Kochia scoparia*), common ragweed (*Ambrosia artemisiifolia*), horseweed (*Conyza canadensis*), palmer amaranth (*Amaranthus palmeri*), and red root pigweed (*Amaranthus retroflexus*).

1.1.1.1. Sub-Objectives

1. Confirm previous greenhouse study findings and generate a weed canopy temperature extraction method for future greenhouse studies.
2. Collect thermal and spectral images of weeds with an unmanned aerial system (UAS) mounted multispectral and thermal imaging system
3. Develop a map of weed populations indicating thermal canopy values and herbicide resistance status

1.1.2. Research Approach

Populations of glyphosate resistant and glyphosate susceptible biotypes of waterhemp, kochia, ragweed, red root pigweed, and palmer amaranth were grown in greenhouse conditions and then subjected to glyphosate application. Thermal values of weed canopies were extracted 1-7 days after treatment and submitted for statistical testing. For the field studies, more populations of weed species were grown and transferred to fields at multiple North Dakota State University Agricultural Experiment Stations (Casselton & Carrington). A randomized complete block design was applied to each species within rows of soybeans that were planted shortly before weed transplantation. A UAS was then used to capture the weed canopies' thermal signatures for further analysis 4, 6, and 8 days after application of glyphosate herbicide as shown in Figure 1.1.

Figure 1.1. Field data collection with DJI M600 UAS

1.1.3. Organization of Thesis

This thesis presents the findings of studies designed to identify glyphosate resistant weeds using thermal sensing technology. Chapter 1 is a literature review detailing various aspects of glyphosate resistance, plant stress, thermal and multispectral imaging, and computational classifiers. Chapter 2 details efforts to validate a previously performed greenhouse study to identify weeds' glyphosate resistance status within a greenhouse setting. Chapter 3 outlines the methodology to perform the greenhouse observation procedure in true field conditions to classify between resistant and susceptible weeds using thermal data as well as multispectral data. References are included at the end of the document.

1.2. Literature Review

1.2.1. Glyphosate Usage

Herbicide usage provides crop producers with multiple benefits including increased crop yield, timely and affordable management, reduced weed pressure, and reduction in soil structure degradation caused by conventional tillage methods (Rahman, 2016). Scientific advancements in the 1990s supported the development of a transgenic glyphosate resistant crop varieties that allowed crop producers to spray herbicides to kill weeds with no concern of harming their crops (Evans et al, 2015). However, dependency on herbicide as a management technique has led to overuse through continuous growth of a single mode of action against resistant crops. In 2010, 93% of all soybeans grown in the USA were herbicide-resistant, as were 78% of all cotton and 70% of all maize varieties (Pollegioni et al., 2011). This rise in herbicide usage is illustrated in Figure 1.2. The overuse of herbicides has caused genetic shifts in weed populations, resulting in resistant biotypes which are difficult to control (Christophers, 1999). Studies estimate that herbicide-resistant management (HRM) has increased herbicide costs in states such as Iowa by $20-$40 per acre from 2013-2017 (Hartzler, 2017).

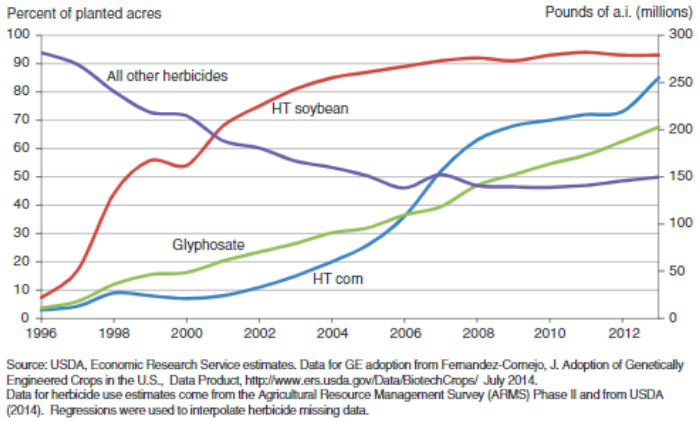

Figure 1.2. Adoption of genetically engineered herbicide-tolerant (HT) corn and soybeans and pounds of herbicide active ingredient (a.i.) applied to those crops, 1996-2013

Glyphosate (N-phosphonomethyl-glycine) is one of the most common herbicides in production agriculture. Developed in 1974, glyphosate is a non-selective herbicide that inhibits the enzyme enolpyruvyl shikimate-3-phosphate synthase (EPSPS) from developing amino acids that are required for protein synthesis (Pollegioni et al., 2011). The interruption of the shikimate pathway is illustrated in Figure 1.3. Additional glyphosate application symptoms include photosynthetic rate reduction, inhibition of growth, and chlorosis of plant tissue (Gomes et al., 2017). The highly effective herbicide quickly established widespread use by crop producers, accelerating the evolution of resistance mechanisms within weeds (Christophers, 1999). Moderate resistance is achieved in some weeds by mutations that occur at the targeted enzyme (Pollegioni et al., 2011). However, glyphosate's translocation through the non-targeted parts of the plants (i.e. plant leaves) reduces the herbicides' ability to reach the root and apical meristems where the inhibition of EPSPS can occur (Pollegioni et al., 2011).

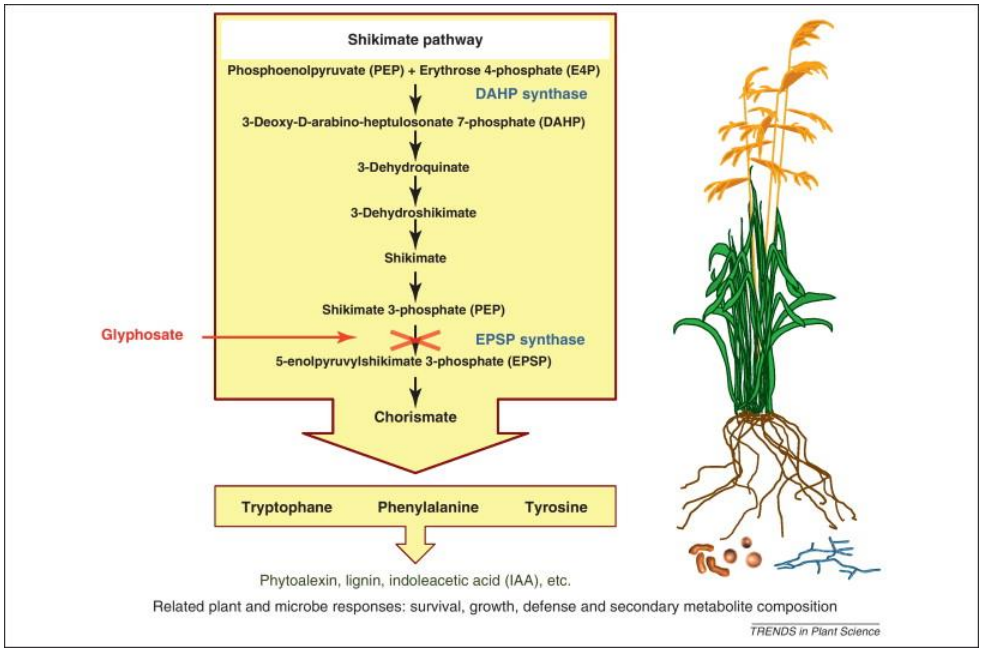

Figure 1.3. Inhibition of EPSP synthesis due to application of glyphosate

1.2.2. Mechanisms of Glyphosate Resistance

In-depth explanation of herbicide resistance requires a complex understanding of weeds' molecular characteristics and how they can adapt to their environment over time. When applying herbicides, there are different modes of action that are enacted upon weeds that instigate mortality (Evans et al., 2010). In the case of glyphosate, the lethal action caused by the herbicide is the inhibition of the enzyme EPSPS. Glyphosate first begins to affect a plant by accumulating in the phloem after it has been absorbed through the parenchymal cells of leaf tissue (Page et al., 2017). The herbicide is then translocated to various parts of the plant where it can invade the growing points of the plant and infect chloroplasts. It is within the chloroplasts that the inhibition of EPSPS occurs. The inhibition of EPSPS results in a blockage in the shikimate pathway which is utilized to create aromatic amino acids (Pollegioni et al, 2011). Shikimate blockage, in turn, does not allow the plant to be able to generate or transport amino acids to other parts of the plant that are dependent upon them for plant survival (Pollegioni et al, 2011).

For a plant to survive a glyphosate application, it must first develop a mode of resistance (also known as resistance mechanism) to glyphosate. Two primary mechanisms of resistance exist within resistant plants. Target-site resistance mechanisms are occurrences where enzymatic mutations occur at the site of action where an herbicide performs its function (Delye et al., 2015). These mutations do not occur in many plant species and multiple factors must be in accordance with each other to facilitate resistance in this fashion. Non-target site resistance is the second class of resistance mechanisms and is most common (Delye et al., 2015). Examples of non-target site resistance include reduced herbicide penetration on the leaf surface, alterations

in translocation within plant that inhibit the plant from reaching the target site, or enhanced metabolic capabilities that reduce the efficacy of the herbicide (Delye et al., 2015).

The physiological basis for weed resistance to glyphosate is complicated and often conferred with varying resistance mechanisms depending on the species in question. In separate studies it was found that an altered EPSPS site was a TSR mechanism responsible for conferring glyphosate resistance in goosegrass while reduced translocation, a NTSR mechanism, was responsible for conferring resistance in annual ryegrass (Green, 2007). The target site mutation conferring resistance in annual ryegrass enacts a transformation of amino acid 106 from proline to serine or threonine that generates a form of resistant EPSPS. This resistant EPSPS enables the annual ryegrass to survive applications of glyphosate (Green, 2007).

Another TSR mechanism, gene amplification, was seen in populations of the closely related waterhemp and Palmer amaranth species where the target enzyme is present in higher concentrations than susceptible plants and therefore is able to endure glyphosate application (Chatham et al., 2015) Gene amplification is also considered to be a prominent mechanism of resistance in kochia as well (Kumar & Jha, 2015). In horseweed, a form of NTSR referred to as compartmentalization was observed where more instances of glyphosate accumulation occurred within vacuoles of resistant plants than susceptible plants (Ge et al., 2010).

Differentiating susceptible and resistant populations of weeds is no easy task. Prior to herbicide application, there is no significant difference in the visual appearance of resistant and susceptible weeds of the same species that can be noticed during scouting (Reddy et al. 2014). Use of hyperspectral systems to detect differences between resistant and susceptible biotypes show potential in controlled environments, but their effectiveness is drastically reduced once introduced to field conditions (Shirzadifar, 2018). Lab testing for an accumulation of shikimic

acid within plant leaves is one method used to identify glyphosate resistance, but its lack of practicality does not justify its use in large scale applications (Xu et al., 2017).

1.2.3. Plant Canopy Temperature

The use of plant canopy temperature data traditionally applies mostly to drought and altered stomatal conductance analysis of crop vegetation (Jones et al., 2009). Leaf temperature is an important variable that impacts the rate of which physiological processes occur within plant tissue (Jones, 2018). Plant canopy temperature is affected by many factors including air temperature, humidity, wind speed, time of day, sky conditions, soil characteristics, and stomatal aperture of the plant species in question (Jones et al., 2009). Canopy temperature is illustrated as a leaf energy balance function in the following equation (Costa et al., 2013).

$$Tcanopy \; - \; Tair \; = \frac{[rHR(raw + rs)\gamma Rni - \rho cprHRVPD]}{[\rho cp\{\gamma(raw + rs) + srHR\}]} \tag{1.1}$$

where

T_{canopy} =plant canopy temperature (K)
T_{air}=air temperature (K),
r_{HR} =parallel resistance to heat and radiative transfer (s m^{-1})
r_{aW} =boundary layer resistance to water vapor (s m^{-1})
γ =psychrometric constant (Pa K^{-1})
R_{ni} =net isothermal radiation (the net radiation for a plant at air temperature) (W m^{-2})
p =density of the air (kg m^{-3})
cp = is specific heat capacity of air (J kg^{-1} K^{-1})
s = the slope of curve relating saturating water vapor pressure to temperature (Pa K^{-1}),
VPD = air vapor pressure deficit

Due to the high amount of environmental variation that dictates this result, many studies have been performed to normalize the environmental variation to mitigate the amount of detailed information that must be gathered to perform the calculation. The various studies have produced a number of indices that do not require such tedious data collection but still maintain validity.

The creation of the crop-water stress index (*CWSI*) by Idso et al. (1982), allowed researchers to investigate plant water relations on a larger scale than previous methods using

$$CWSI = (T_s - T_{nws})/(T_{dry} - T_{nws}) \quad (1.2)$$

where

Ts = leaf canopy temperature
Tnws = temperature of a watered canopy transpiring at its potential rate

This index has been widely used for crop irrigation scheduling and also benefits from the fact that variations in atmospheric humidity (which can negatively impact index results) are accounted for (Jones, 2018). A variation to the CWSI was developed by Jones (1999) resulting in the index of stomatal conductance (I_g) alternatively using

$$I_g = (T_{dry} - T_s)/(t_s - T_{wet}) \quad (1.3)$$

where

Twet = temperature of a wet reference surface
Tdry = temperature of a non-transpiring reference surface

The result of this formula is proportional to stomatal conductance (g_1) and therefore can be further converted to stomatal conductance using the following equation (Jones, 2018).

$$g_l = I_g/(r_{aW} + (s/\gamma)r_{HR}) \quad (1.4)$$

Stomatal conductance is a measure of the degree of stomatal opening of plant leaves and is often used as an indirect indicator of plant-water status. Stomatal conductance is lessened in during water stress situations to mitigate transpiration and conserve water within the plant tissue. The inhibition of stomatal conductance results in increased leaf temperatures due to the loss of water and eventual desiccation of leaf vegetation. (Gimenez et al., 2013)

1.2.4. Thermal Imaging of Glyphosate-Affected Vegetation

Thermal imaging has proven itself to be an invaluable method to collect canopy temperature data. Compared to other thermal collection systems such as IR thermometers or thermocouples, thermal cameras allow the user to better understand the variance of temperature of any object, including vegetation (Jones, 2018). Thermal imaging has shown potential in detecting plant canopies experiencing increased levels of stress and reduced photosynthesis (Stoll and Jones, 2007). The application of glyphosate to susceptible plants causes a reduced photosynthetic rate due the inhibition of stomatal conductance (Picoli et al., 2016). The reduction in stomatal activity lowers the transpiration of water throughout the plant leaf, resulting in increased leaf temperature (Gonzalez-Dugo et al., 2019). If the affected plant canopy emits a significantly higher temperature, there is potential for the temperature change to be visualized by a thermal imager.

Historically, thermal images of landscapes were primarily captured using satellites that provided low-resolution (10m+) which were only suitable for large scale applications to monitor regional drought and detect plant water stress in dense vegetation (Veysi et al., 2017). The introduction of newer, higher resolution thermal imaging systems that are compatible with unmanned aerial vehicles (UAV) have boosted the practical use of thermography within agriculture. The enhanced resolutions have enabled crop producers to record and manage water stress on a smaller scale than with satellite imagery, thus reducing operating costs by mitigating over-irrigation (Gonzalez-Dugo et al., 2015). Recent studies have demonstrated the relatively untapped potential of thermal imagery to conduct high-throughput plant phenotyping. Maimaitijiang M. et al. (2017) found that a combination of multispectral and thermal data provided a high quality estimate for nitrogen concentration and chlorophyll content of soybeans.

Ludovosi et al. (2017) compared drought response of 503 genotypes of black poplar trees to designate drought-tolerant varieties of black poplar trees. Thermal imaging has also been successfully utilized to estimate wheat yields by monitoring average canopy temperatures (Guo et al., 2016).

1.2.5. Multispectral Imaging Technology

Analogous to thermal sensing, multispectral sensing is also used extensively within agriculture. Multispectral sensing is the practice of using one sensor to image multiple areas of the light spectrum at the same time (Micasense, 2017). When paired with UAV, multispectral sensing payloads have proven to be powerful detectors of biophysical characteristics of vegetation during the growing season (Liu et al., 2018). Multispectral cameras capture image data within specified wavelengths of the electromagnetic spectrum, most commonly in the blue, green, red, red-edge, & near-infrared wavelengths. But some sensors such as the Micasense Red-Edge MX Dual Camera is capable of capturing as many as ten different wavelengths at the same time (Micasense, 2020).

The high spatial and spectral resolution can be used for a variety of agricultural applications including high-throughput phenotyping, disease identification and severity analysis, nutrient management, and weed identification and mapping (Micasense, 2020). Rapid identification of plant height, canopy cover, vegetation index, and flowering stage was performed in cotton fields to enhance breeding using multispectral images over multiple stages of the growing season (Xu et al., 2019). Potato late blight disease severity was measured using leaf and canopy measurements from the red and red-edge wavelengths with classification accuracies as high as 89.33% (Fernandez et al, 2020). Optimal, site specific, nitrogen fertilizer rate was investigated by Thompson and Puntl (2020). Their use of multispectral sensors reduced

nitrogen application rates by approximately 31 kg N ha^{-1} without causing yield losses and improved nitrogen use efficiency by as much as 18%. Finally, computational deep learning with multispectral images provided a practical solution to identifying weeds in a sugarbeet field by detecting subtle differences in shapes and reflectance patterns of their leaf canopies (Dyrmann et al., 2018).

1.2.6. Image Based Machine Learning Classification Methods

Traditional methods of computationally differentiating agricultural data utilizes machine learning. Machine learning is generally separated into two classes, supervised and unsupervised. Supervised learning develops a predictive model based on a subset of the data inspected intensely ("trained") by a computer and then used to predict untrained data status. Unsupervised learning does not require the need for training and is useful for finding patterns within datasets (Matlab, 2020).

Support vector machine modeling is a form of supervised machine learning designed to analyze and separate classes within datasets based upon the characteristics of training examples provided to it (Furey et al. 2000). A hyperplane is generated to classify and segregate data points into their respective classes. The hyperplane location within the dataset depends on the presence of support vectors, which are data points that prove to be the most difficult to classify. The identification of support vectors optimizes hyperplane generation and maximizes the margin between datasets, leading to more reliable classifications (Shi et al., 2012).

Another common classification method is random trees, a set of individual decision trees where each tree is generated from subsets of the training data (ESRI, 2020). A decision tree is a set of determinants listed by priority with the goal of coming to a final decision which designates the untrained data as one class or another (ESRI, 2020).

2. IMAGE BASED THERMAL SENSING FOR GLYPHOSATE RESISTANT WEED IDENTIFICATION IN GREENHOUSE CONDITIONS

2.1. Introduction

In 2019 and 2020, greenhouse studies were performed with the objective of validating and improving a previously developed method to distinguish between herbicide resistant and herbicide susceptible weeds. In these studies, six weed species were included; waterhemp, kochia, ragweed, horseweed, palmer amaranth, and red root pigweed. The weeds selected were determined to be most relevant to North Dakota agriculture and showed the most potential for herbicide resistance. The stepwise regression and SVM classification strategies were utilized to validate the findings of Shirzadifar (2018) and one tailed t-testing to examine the significance of the temperature differences observed. However, modifications were made to the data collection procedure in an attempt improve the thermal signature selection procedure to provide the SVM classifier with the most accurate information possible while adhering to the original method as much as possible.

2.2. Materials and Methods

2.2.1. Species and Biotype Selection

This experiment was performed in a greenhouse at North Dakota State University in Fargo, ND. Seed collections were gathered for two biotypes of waterhemp (Figure 1.a), kochia (Figure 1.b), ragweed (Figure 1.c), horseweed (Figure 1.d), palmer amaranth (Figure 1.e) and red root pigweed (Figure 1.f) to perform the experiments. The biotypes chosen were based on their resistance to glyphosate application with the goal of having one biotype serve as a resistant population, and another biotype serves as a susceptible population. To test for resistance, small samples of each biotype were grown in 4-inch plastic pots and treated with a glyphosate-based

herbicide solution. Survival evaluations of these tests contributed to the selection of the biotypes. The seeds were sourced from various locations throughout the contiguous United States of America.

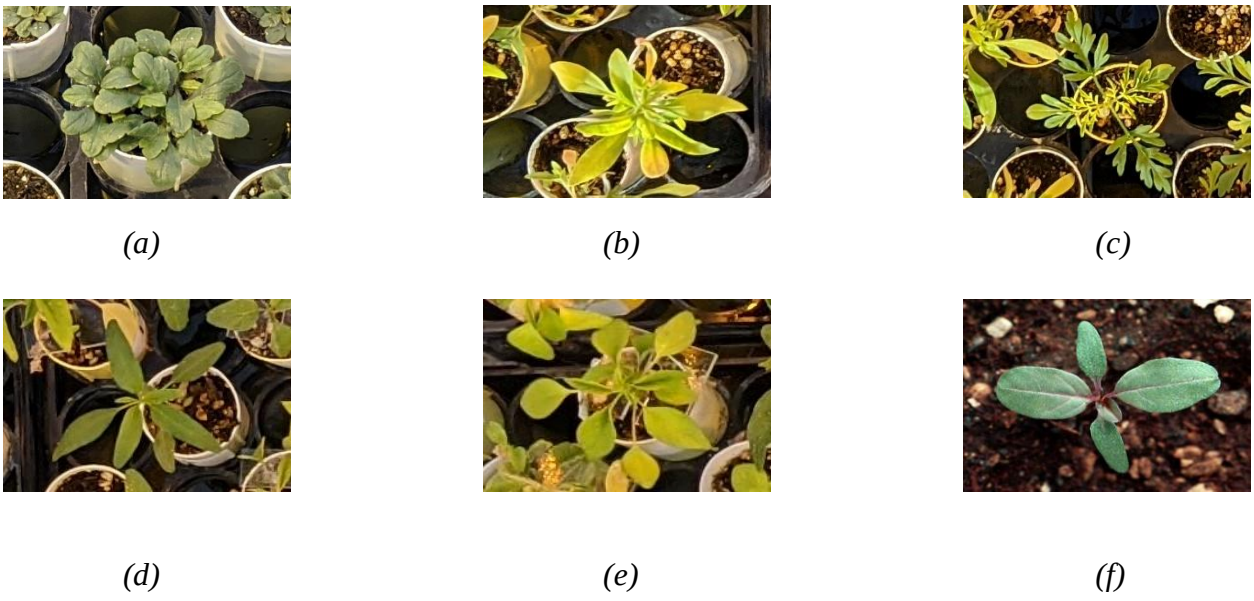

(a) *(b)* *(c)*

(d) *(e)* *(f)*

Figure 2.1. Images of weed species. a) horseweed, b) kochia, c) ragweed, d) waterhemp, e) Palmer amaranth, and f) redroot pigweed

2.2.2. Weed Planting & Growing Conditions

Seeds from each species were planted in Ray Leach SC10 Super cone-tainer cells (Stuewe & Sons Inc., Tangent, OR, USA) with a cell diameter of 3.8 cm and a depth of 21 cm (1.5" diameter, 8.25" depth). The cells were filled with commercial potting mix (Metro-Mix 360; Sun Gro Horticulture, Bellevue, WA) and seeds were planted and separated based upon biotype. Cone cells were placed in 70×30.5×17.15 cm^3 racks which held the potting mix for the weeds. Plants were watered overhead by hand until reaching a height of approximately 10cm, after which they were placed in sub-irrigation tubs for the duration of the experiment. To perform the experiment, a space of approximately 1.5×1.0 m^2 was utilized to accommodate the weeds during monitoring. The greenhouse temperature was set to 21° C for the duration of the

experiment. From 06:00 h to 20:00 h each day, additional heat and light were provided by sodium vapor lamps as well as natural light to provide a 14 h photoperiod. In 2019, all six weed species were grown and observed simultaneously. In 2020, the horseweed experiment was grown and performed independently due to poor germination occurring on the first attempted experiment, while the kochia was paired with ragweed and Palmer Amaranth was paired with waterhemp to gather data for all species while maintaining a concise experiment timeline.

2.2.3. Application of Glyphosate and Thermal Monitoring Setup

Once the height of the weeds averaged approximately 10 cm, the weeds were treated with Roundup PowerMax herbicide (Monsanto Company, St. Louis, MO) in a concentration of 1.7ml herbicide to 100ml H_2O (1.7%) within a cabinet sprayer (DeVries Manufacturing, Hollandale, MN, USA, Figure 2.2.). The herbicide applications were performed at 40 psi at 1.33 m/s with a boom height of 41.3 cm. The herbicide was paired with 0.25 ml of nonionic surfactant and 1.019 g of ammonium sulfate adjuvant to ensure even coverage.

Figure 2.2. DeVries cabinet sprayer

To monitor the canopy temperature of the weeds post-herbicide application, an ICI Model 9640 P-series (Infrared Cameras Incorporated, Beaumont, TX, USA) thermal camera was

used to capture one thermal image of the experiment area per hour up to 110 hours (4.5 days). The ICI thermal camera was equipped with a 25mm manual focus lens that provided a 24.8°×18.6° field of view. It stored long wave infrared (LWIR) (7-14µm) images in a 640×480 pixel array for visualization. To operate the camera and convert the LWIR values to temperature values, the computer software IR Flash (Infrared Cameras Incorporated, TX, USA) was used on a laptop using the Microsoft Windows 7 operating system.

Prior to image collection, it was necessary to ensure that the camera was recording accurate temperature values. A Blackbody ICI 350 Portable IR Calibrator (Infrared Cameras Incorporated. TX, USA) and a handheld IR thermometer (Model Raynger ST-4, Raytek. Wilmington, NC, USA) were used to check the calibration of the ICI thermal camera. Figure 2.3 displays the results of a calibration experiment to test the accuracy of the camera. Upon reviewing the high R^2 returned by plotting the results, it was determined that the camera satisfied the performance required to conduct the experiment.

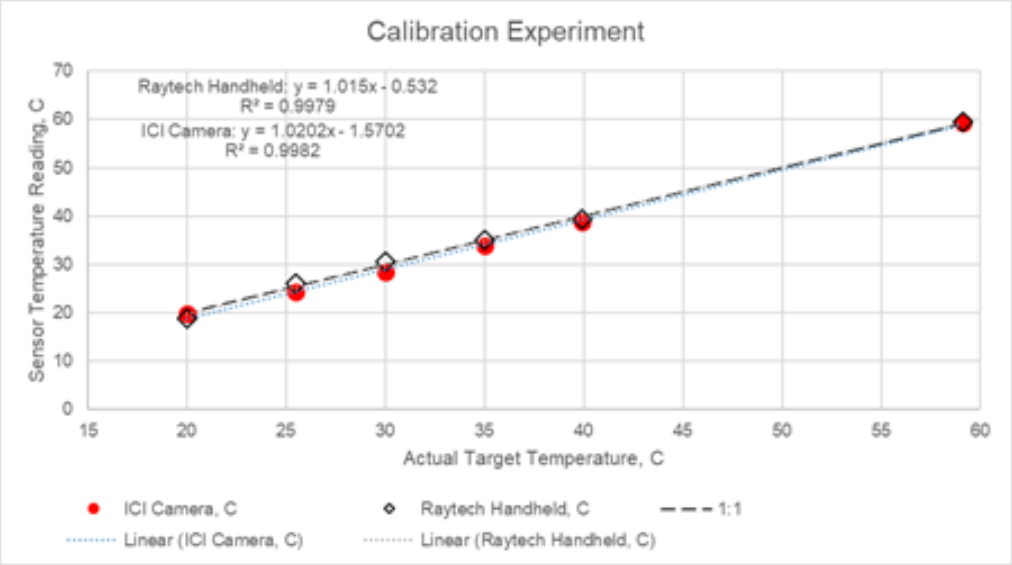

Figure 2.3. Accuracy of ICI camera with ICI Blackbody providing Actual Target Temperature

The ICI thermal camera was mounted 1.83 m (6 feet) above the surface of the experiment area on a cross beam throughout the experiment. At this height, the camera provided 2.0 mm spatial resolution (Fig. 2.4).

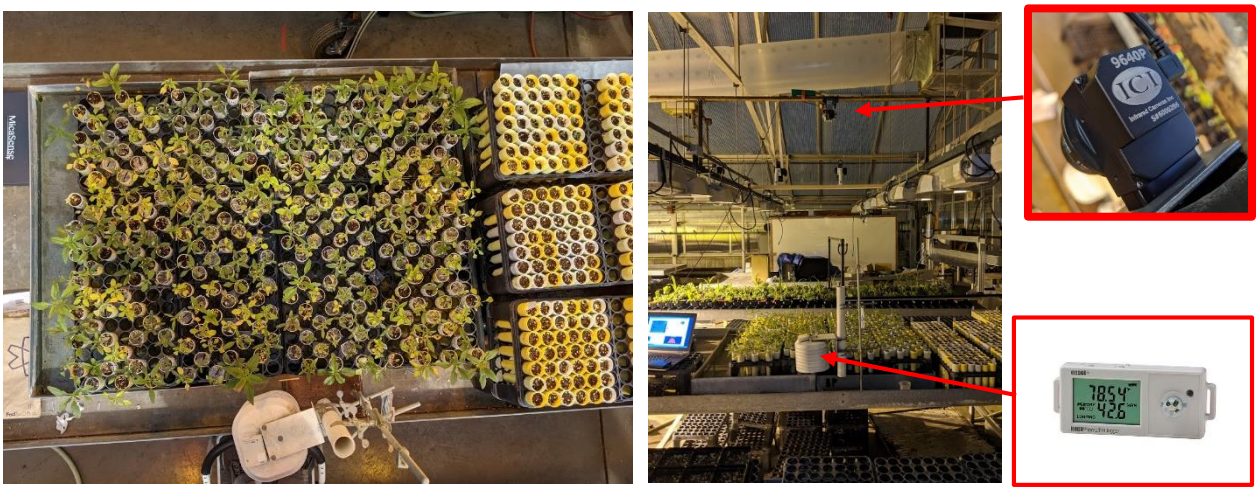

Figure 2.4. Layout of thermal monitoring station while monitoring waterhemp and Palmer amaranth with close-up images of ICI 9640p thermal camera and HOBO temperature logger

To account for variations in environmental conditions, a HOBO pro series sensor (Onset MA, USA) was used to collect temperature, relative humidity, and light intensity data of the experiment area. The temperature data collected by the sensor is a critical component in the analysis of thermal images because the ambient temperature significantly impacts the canopy temperature of the weeds. The ambient temperature is also a factor in the expression $T_{Canopy} - T_{Air}$ which is used to calculate the differences between weed species biotypes and to estimate stomatal conductance within plants (Jones et al., 2009).

2.2.4. Experimental Layout

Experimental layout between the test years of 2019 and 2020 varied. In 2019, position of resistant and susceptible biotypes were randomized on a greenhouse bench. Visible observations were made 14 days after application to confirm resistance status of samples based upon their degree of herbicide symptomology. Thermal values from 34 samples of either susceptible or

resistant were compared using one tailed t-tests for each hour of data collection for each tested species.

In 2020, population sizes were increased. To optimize the distinction between glyphosate susceptible and resistant biotypes, sampling was performed for weeds that could be easily categorized as susceptible or resistant based upon visible observation. Therefore, the number of sampled plants was less than the total number of plants within the experiment area. The horseweed experiment was performed independently of other species and the randomization between biotypes was repeated. It was found that 42 horseweed plants were susceptible to the glyphosate treatment and 40 were resistant. (Fig. 2.5) In the kochia and ragweed experiment, 50 resistant and 45 susceptible kochia plants were sampled and 50 resistant and 50 susceptible ragweed plants were sampled. The waterhemp and Palmer amaranth experiment contained 40 resistant and 43 susceptible waterhemp plants samples with 48 resistant and 38 susceptible Palmer amaranth samples, respectively.

Figure 2.5. Comparison of glyphosate resistant (left) and glyphosate susceptible (right) horseweed

2.2.5. Thermal Signature Extraction Process

A novel method of extracting thermal values from images was developed to accommodate this study. Once images were captured using the ICI thermal camera, thermal

images were exported to CSV format. Matlab software (version 9.4, MathWorks, Santa Clara, CA) was used to further process the images. A script was made to upload all thermal datasets from an experiment and arrange (or 'stack') them in a 640x480xHI multiway array relating to row pixel, column pixel, and (HI) hourly images, respectively. (Fig. 2.6)

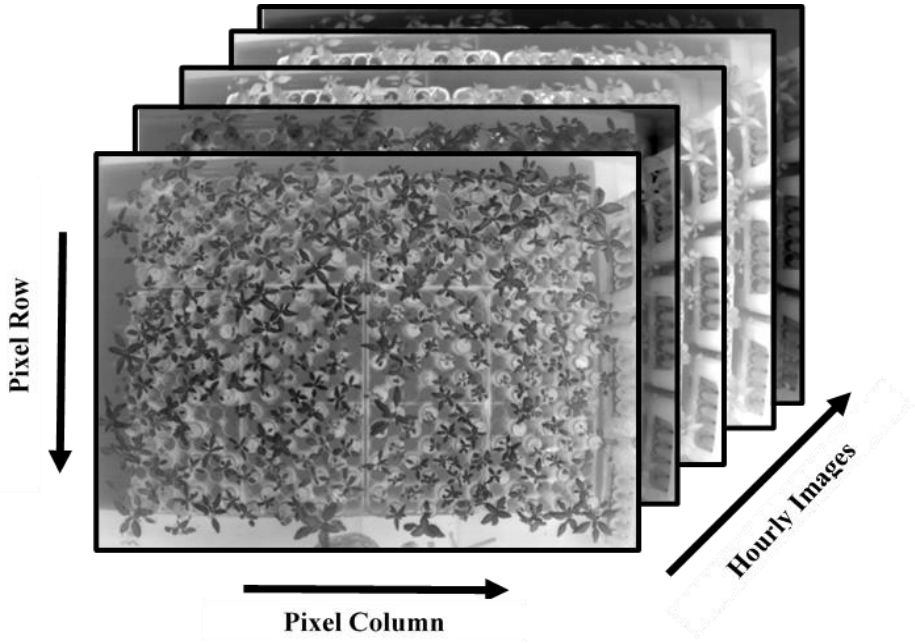

Figure 2.6. Visual representation of multiway array assembly

Manual selection of plant locations on a template image were used to crop these larger images into plant sample multiway arrays. The dimensions of this array is described as

$$(Length\ of\ Sample\ Image \times Width\ of\ Sample\ Image \times No.\ of\ Images\ Captured \times No.\ of\ Sampled\ Plants)$$

Finally, a manual sampling procedure was used to extract ten, single pixel thermal value samples from each cropped weed canopy at every hour to form aggregated datasets of resistant and susceptible canopy temperatures up to 113 hours after application of glyphosate for use in regression modeling (Figure 2.7.).

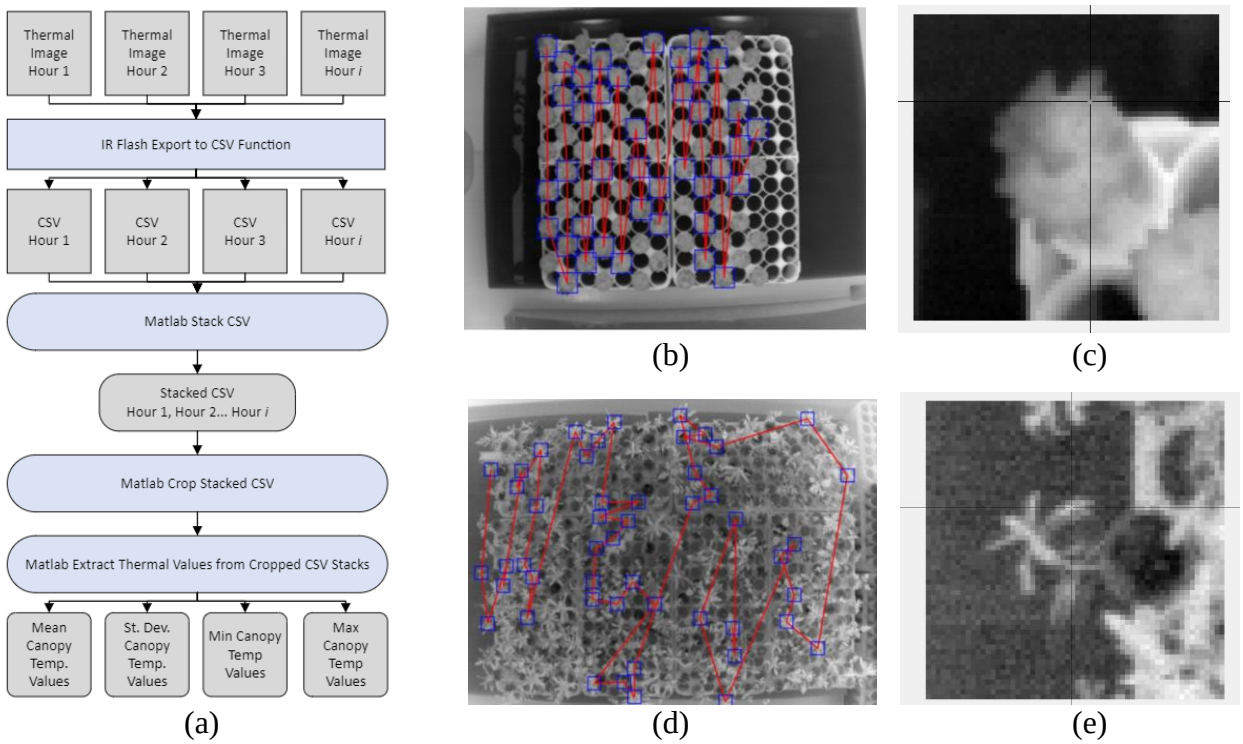

Figure 2.7. Thermal signature extraction procedure. a) Flowchart of operations b) Selection map for resistant horseweed where blue boxes denote areas of CSVs that were cropped and used for canopy temperature retrieval; c) Example of cropped resistant horseweed where black crosshairs indicate which pixel value was recorded for final datasets d)Selection map for susceptible kochia e)Example of cropped susceptible kochia

To normalize the temperature values of the weeds, the equation $T_{Canopy} - T_{Air}$ was used. Where, T_{Canopy} is the value observed by the ICI thermal camera and T_{Air} is the value observed by the HOBO sensor. This allowed differences in temperatures to occur along an equivalent range, so that the data can be used in regression modeling and machine learning models.

2.2.6. Statistical Analysis of Weed Canopy Differences

The datasets assembled using the extraction method were subjected to multiple statistical tests. A one tailed t-test (a= 0.05) was performed for each tested species for every hour of

collected data to test the alternative hypothesis that glyphosate susceptible plants exhibit canopy temperatures that are significantly higher than glyphosate resistant plants.

A stepwise regression function was then used to identify the hour after glyphosate application in which the distinction between resistant and susceptible crops was most prevalent. In this instance, the canopy temperatures collected each hour, after glyphosate application, served as the potential predictor variables. Variables were considered significant at an alpha value of 0.05. Variables having a probability of a greater F of greater than 0.1 were not considered. Model performance was then illustrated by observing the adjusted coefficient of determination and standard error of the estimate.

Finally, the datasets were used for training a linear SVM classification model. The datasets for each species were then submitted to a support vector machine classifier, where 70% of the plants served as training data to classify the remaining 30% as glyphosate susceptible or resistant plants. The predictor variables collected during the stepwise regression procedure were utilized as support vectors for the classification procedure to aid in the classification of glyphosate resistant weeds. Classification results were then investigated using several performance metric methods the assess the agreement between the classified results and the actual weed herbicide resistance statuses.

2.3. Results and Discussion

2.3.1. Plant Canopy Temperature of Glyphosate Resistant and Susceptible Weeds

The mean canopy temperatures of each biotype included in the experiment were grouped according to their respective species type and plotted to create a generalized comparison of canopy temperature differences. In 2019, no easily discernable difference occurred in any of the tested species (Figure 2.8.). However, upon closer evaluation it was seen that resistant kochia

and waterhemp maintained consistently lower temperatures throughout the data collection period than the susceptible biotypes albeit minute differences at best.

In 2020, waterhemp, Palmer amaranth, kochia, and ragweed all exhibited temperature signatures that showed little difference in canopy temperature between biotypes (Figure. 2.9.). However, horseweed displayed a window of increasing differences between resistant and susceptible plants beginning roughly 60 hours after herbicide application (Figure 2.9.a). This is the only finding that showed similar trends to Shirzadifar (2018).

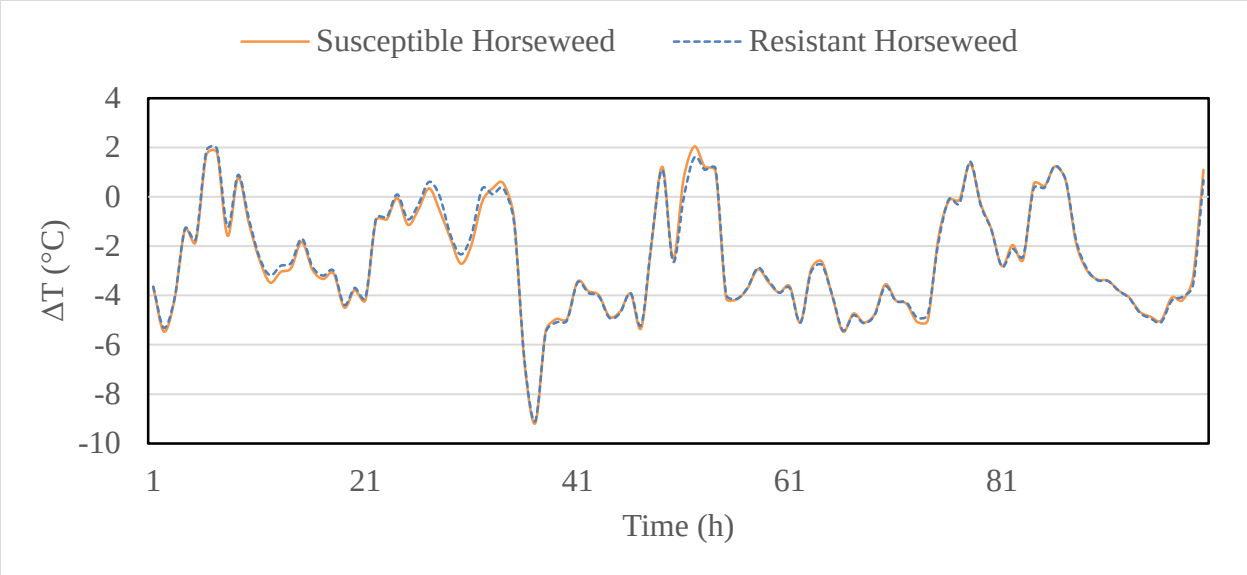

(a)

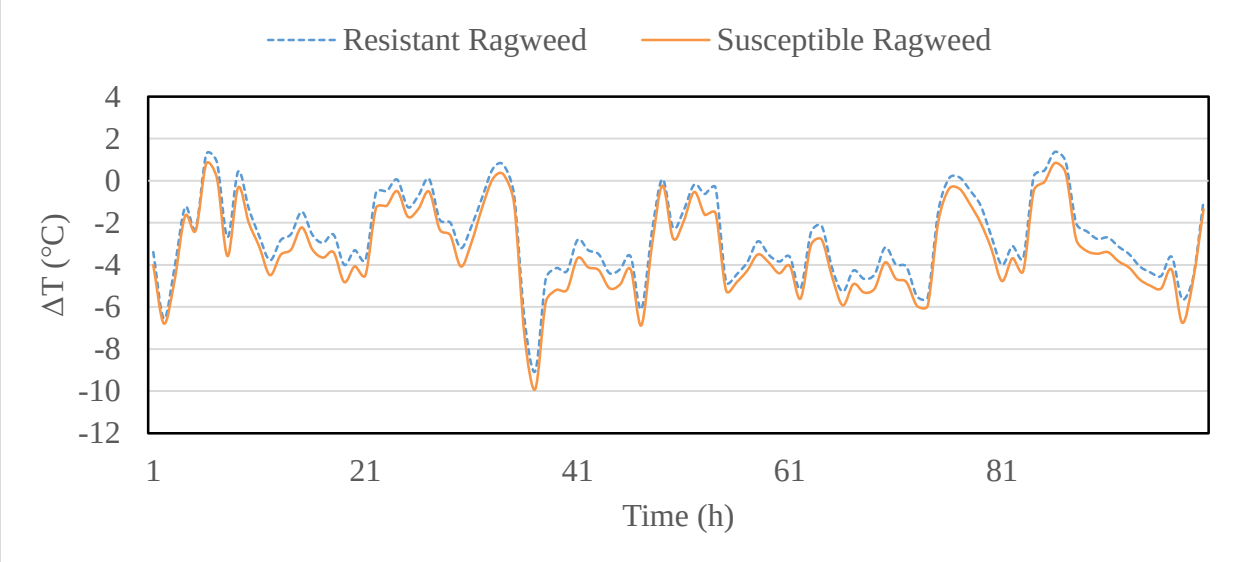

(b)

Figure 2.8. 2019 Experiment: Differences between plant canopy thermal signatures and ambient temperature of glyphosate resistant and glyphosate susceptible weeds. a) horseweed, b) ragweed, c) kochia, d) Palmer amaranth, e) waterhemp, and f) red root pigweed

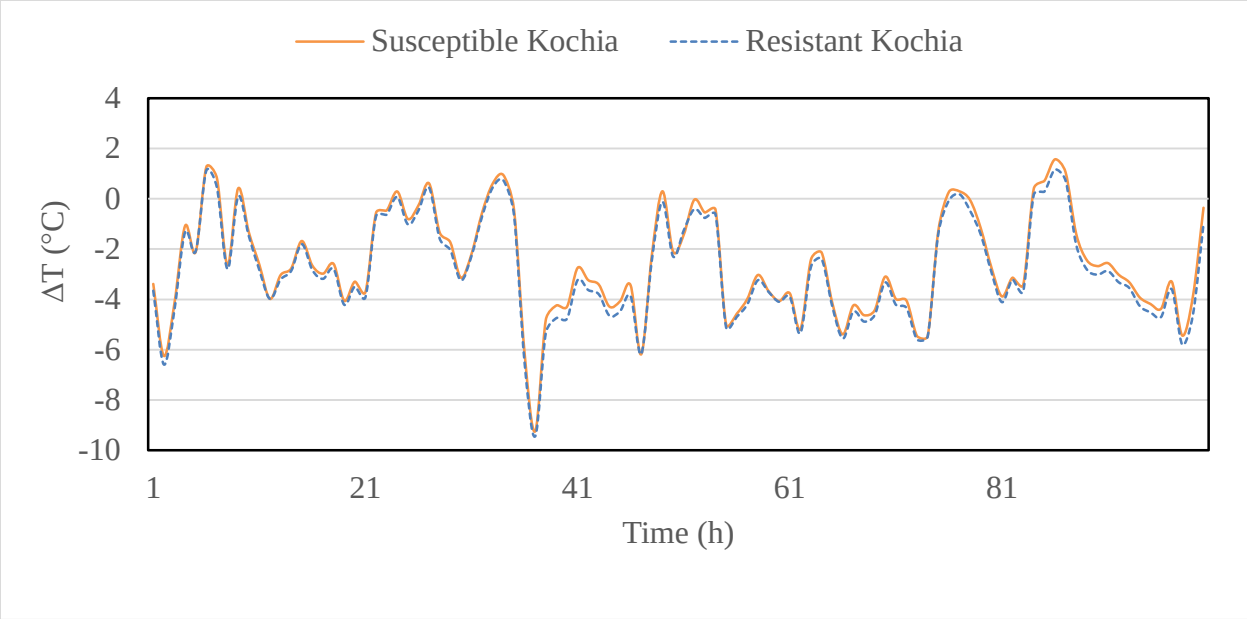

(c)

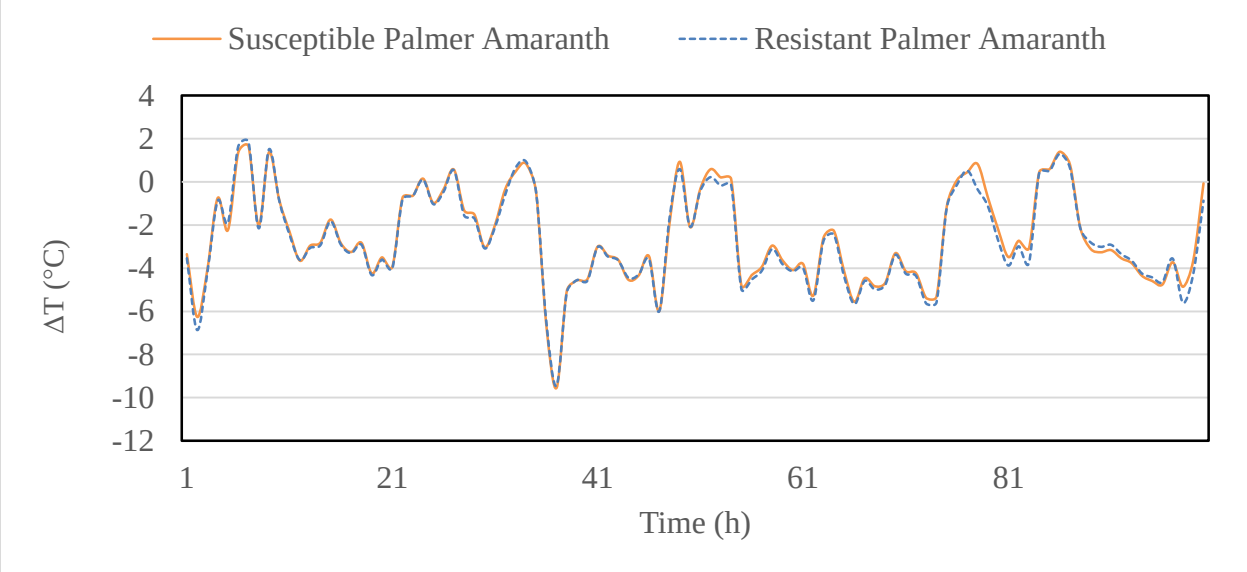

(d)

Figure 2.8. 2019 Experiment: Differences between plant canopy thermal signatures and ambient temperature of glyphosate resistant and glyphosate susceptible weeds. a) horseweed, b) ragweed, c) kochia, d) Palmer amaranth, e) waterhemp, and f) red root pigweed (continued)

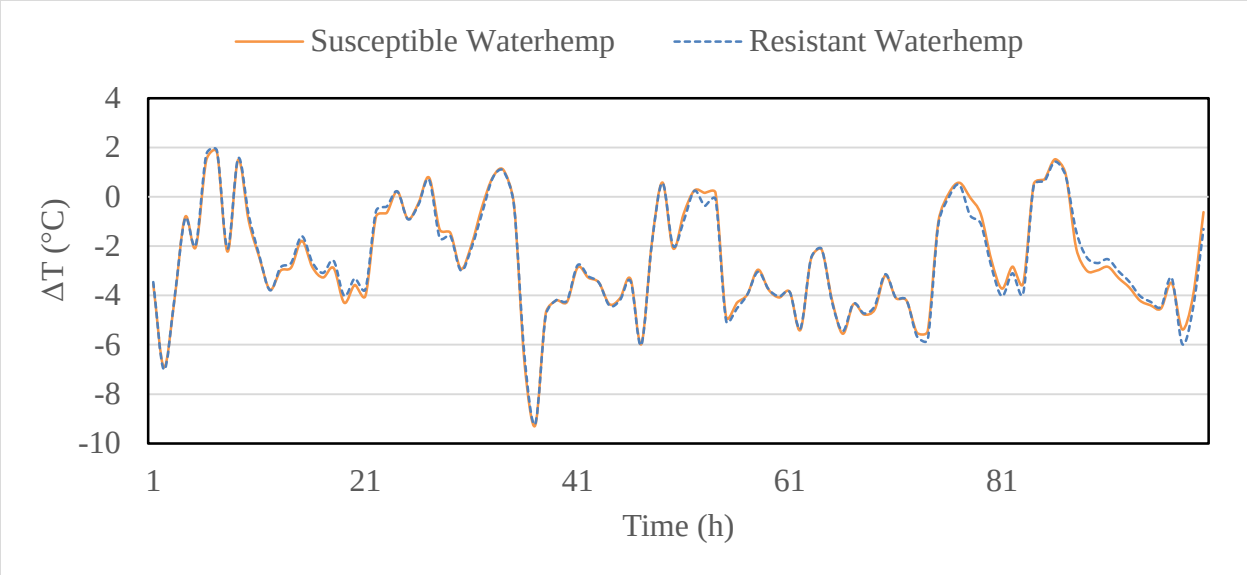

(e)

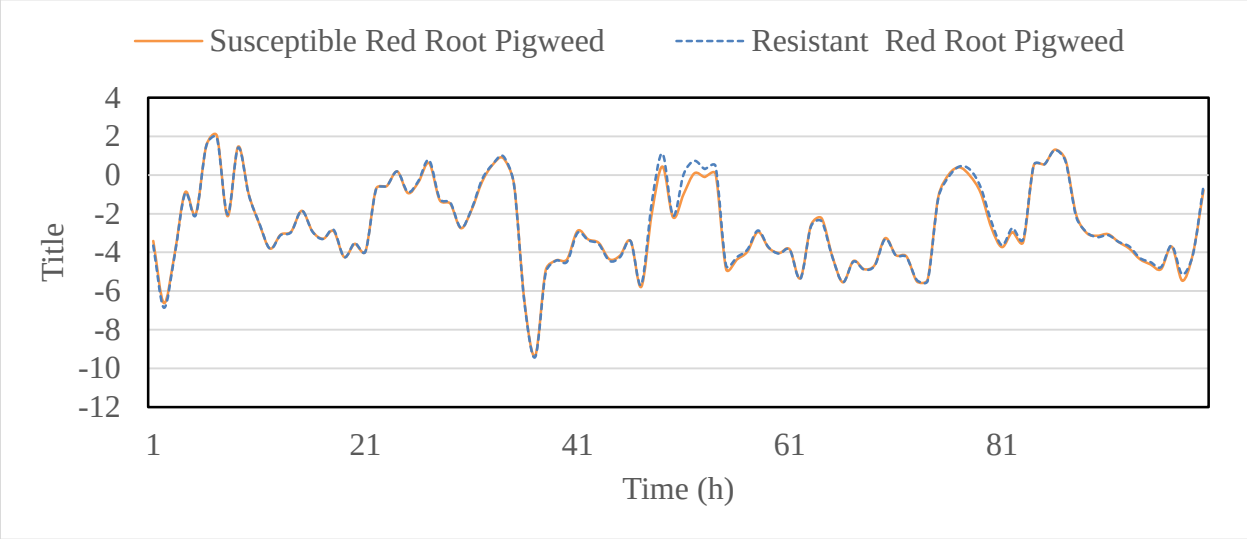

(f)

Figure 2.8. 2019 Experiment: Differences between plant canopy thermal signatures and ambient temperature of glyphosate resistant and glyphosate susceptible weeds. a) horseweed, b) ragweed, c) kochia, d) Palmer amaranth, e) waterhemp, and f) red root pigweed (continued)

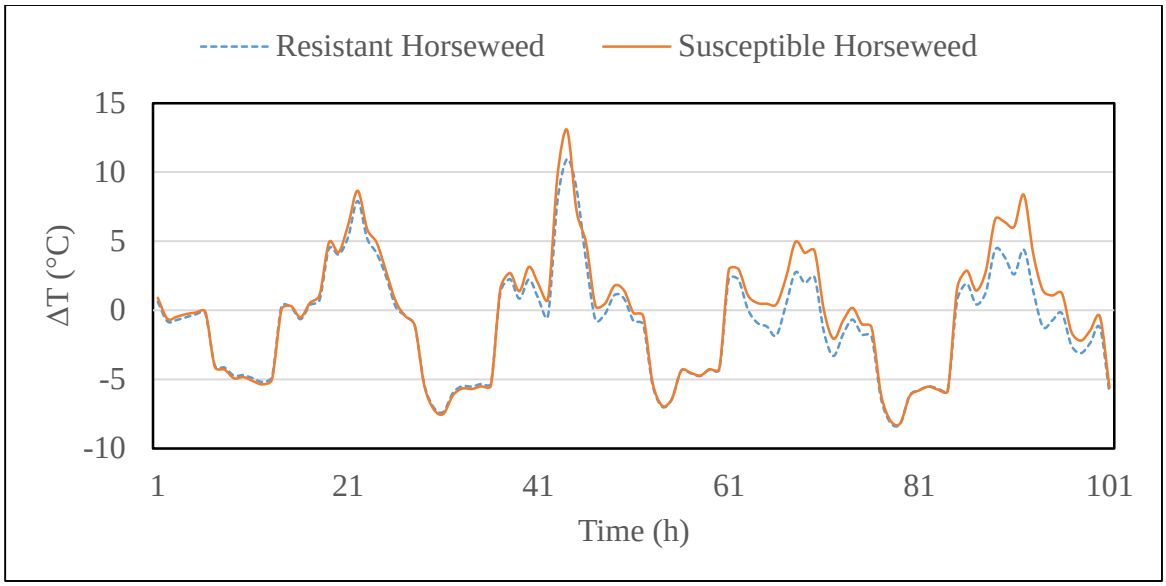

(a)

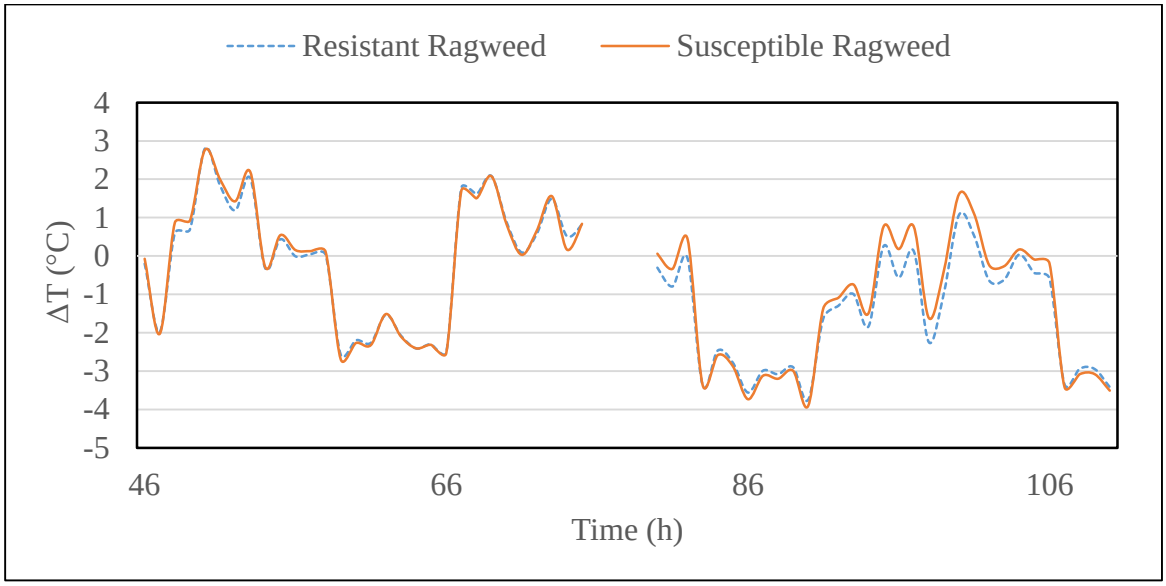

(b)

Figure 2.9. 2020 Experiment: Differences between plant canopy thermal signatures and ambient temperature of glyphosate resistant and glyphosate susceptible weeds. a) horseweed, b) ragweed, c) kochia, d) Palmer amaranth, and e) waterhemp. Camera malfunction caused loss of data from 1-46 hours and 76-79 hours after glyphosate application in kochia and ragweed

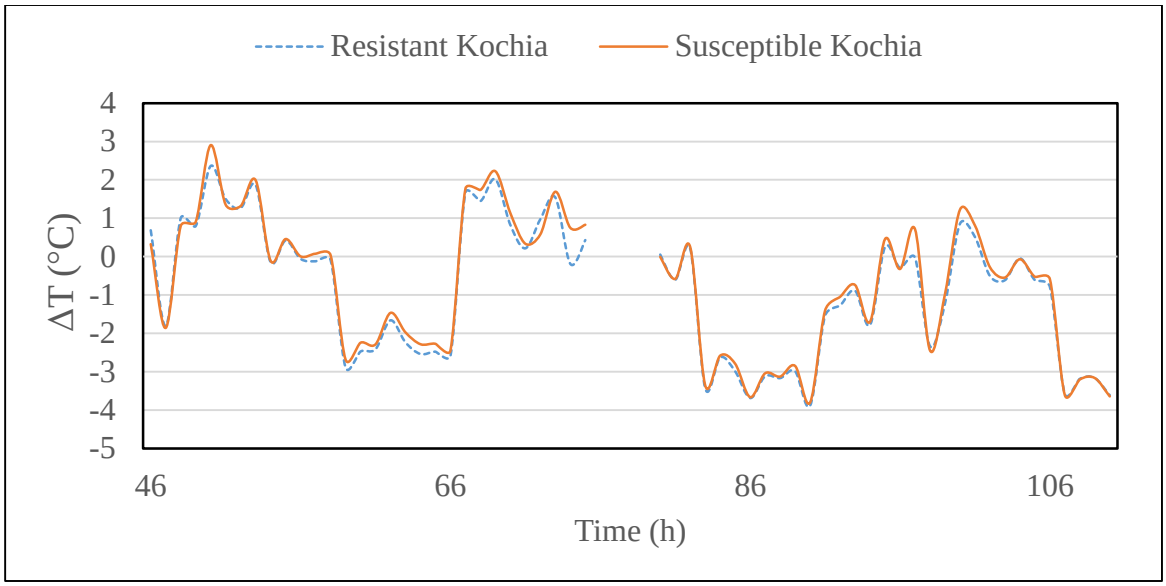

(c)

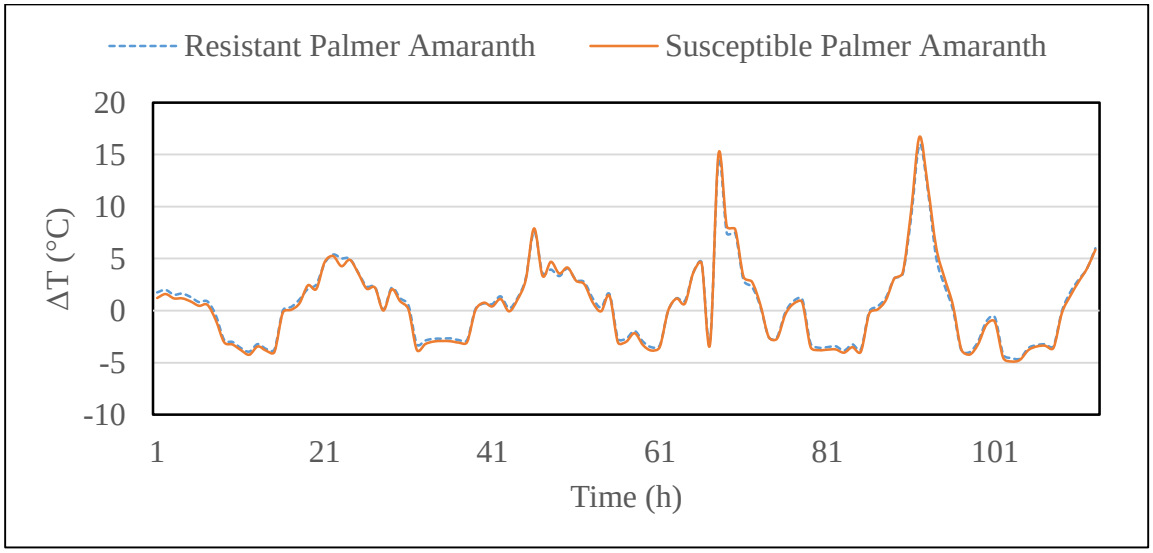

(d)

Figure 2.9. 2020 Experiment: Differences between plant canopy thermal signatures and ambient temperature of glyphosate resistant and glyphosate susceptible weeds. a) horseweed, b) ragweed, c) kochia, d) Palmer amaranth, and e) waterhemp. Camera malfunction caused loss of data from 1-46 hours and 76-79 hours after glyphosate application in kochia and ragweed (continued)

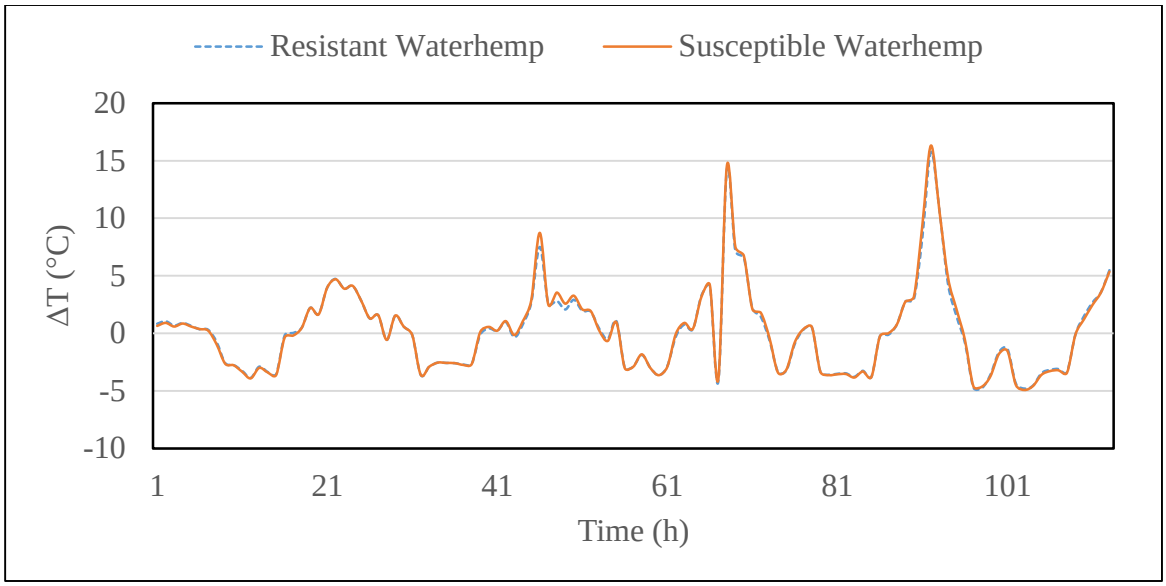

(e)

Figure 2.9. 2020 Experiment: Differences between plant canopy thermal signatures and ambient temperature of glyphosate resistant and glyphosate susceptible weeds. a) horseweed, b) ragweed, c) kochia, d) Palmer amaranth, and e) waterhemp. Camera malfunction caused loss of data from 1-46 hours and 76-79 hours after glyphosate application in kochia and ragweed (continued)

While biotypes of species were screened for their susceptibility or resistance prior to evaluation, the biotypes of kochia, ragweed, Palmer amaranth, and waterhemp showed mixed response to the glyphosate application. Visible evaluations were performed 14 days after application (Table 2.1.). Directed sampling was performed to include weeds that were highly susceptible or resistant. However, in order to maintain valid population sizes for further testing, some plants were selected that . During the experiments, every weed was categorized on a scale of 0-5 to describe the magnitude of their resistance (MoR). Plants with a MoR less than or equal to 2 were classified as susceptible and plants with an MoR greater than or equal to 3 were classified as resistant.

Table 2.1. Individual Plant Survival Evaluation from Application of Glyphosate

	Magnitude of Resistance						# Observed		# Sampled for Testing	
Species	0	1	2	3	4	5	Susc.	Res.	Susc.	Res.
Horseweed	42	0	0	0	0	40	42	40	42	40
Kochia	16	20	20	40	24	29	56	93	45	50
Ragweed	27	30	37	25	10	15	94	50	50	50
Waterhemp	2	11	30	58	39	4	43	101	43	40
Palmer amaranth	21	16	42	40	7	1	79	48	38	48

Magnitude of Resistance Key: 0=Dead Plant 5=Alive Plant with no Symptoms

The distinction between glyphosate resistance and susceptibility that occurred in biotypes of horseweed, but not in other species, seems to connect with the low canopy temperature differences observed in Figure 8. The 42 horseweed plants that were selected for high susceptibility to glyphosate successfully succumbed to the herbicide treatment and were given an MoR of 0 or 1. Meanwhile, the 40 horseweed plants that were selected for resistance traits displayed great resistance to the herbicide treatment and all of them were granted an MoR of 5. This distinction could possibly offer reasoning as to why differences in average canopy temperatures are noticeable within Figure 2.9.a. This level of distinction did not occur in kochia, ragweed, waterhemp, or Palmer amaranth, where a large number of plants were classified with a MoR of 2 or 3 therefore resulting a great deal of indefinite observations. When sampling for testing, plants with an MoR of 2 or 3 were avoided, but some selections had to be made to ensure adequate sample sizes for further use in classification models.

Therefore, the inclusion of plants that showed mixed response to glyphosate possibly caused the differing results of this study compared to Shirzadifar (2018) findings where large temperature differences existed as early as 10 hours after application in kochia, ragweed, and waterhemp. The ratio of susceptible to resistant plants was not reported by Shirzadifar (2018), therefore no direct comparison can be made to strengthen the suggestion that varied levels of resistance deter the effectiveness of observing thermal values to determine glyphosate resistance.

However, the inclusion of weeds with different degrees of resistance is suggested by Shirzadifar (2018) as potential future research, so the presence of variably resistant weeds in this study actually introduces valuable insight into the overall practicality of the method. By observing the small differences recorded from weeds with varying MoRs, it can be seen that the inhibition of stomatal conductance and increased canopy temperatures cannot be seen as easily as compared to weeds with large differences in MoR.

2.3.2. One Tailed t-Test Analysis and Interpretation

In 2019, all t-tests executed to test if plants with glyphosate susceptibility exhibited significantly higher canopy temperatures than resistant plants returned results that disputed the alternative hypothesis. Over the course of the experiments, neither kochia, ragweed, or red root pigweed showed any instances where their susceptible temperatures were significantly higher than their resistant counterparts. Only 2 out of 100 tests of susceptible Palmer amaranth and 1 out of 100 tests of horseweed were significantly higher temperature than resistant weeds at level $\alpha = 0.05$, confirming that canopy temperatures of the populations of susceptible plants were not significantly higher than resistant plants after glyphosate application.

In 2020, the t-test returned multiple results that dispute the alternative hypothesis. Throughout the experiments, only 1 out of 113 tests of susceptible Palmer amaranth was significant at level $\alpha = 0.05$, strongly suggesting that canopy temperatures of susceptible plants are not significantly higher than resistant plants after glyphosate application. Within kochia and waterhemp, larger differences tended to be found between resistance classes compared with Palmer amaranth but still failed to reject the null hypothesis of no differences. Only 8 out of 65 tests of susceptible kochia were classified as significant at significance level $\alpha = 0.05$ while waterhemp had 12 significant tests of 113 total. Some differences existed in ragweed as 16

significant tests were found out of 65 recorded tests at $\alpha = 0.05$. All of the significant tests in kochia, waterhemp, and ragweed occurred 60 hours after application, indicating that the difference in temperature between susceptible and resistant biotypes before 60 hours were indistinguishable. None of the tests within kochia, ragweed, waterhemp, or Palmer amaranth satisfied the Bonferroni adjusted level of significance ($\alpha = 0.05/100$ where 100 represents the total number of tests performed). Glyphosate visual symptomology typically begins 48-96 hours after application (Monsanto Company, 2017) Therefore, the onset of visual symptoms after glyphosate application is expected to occur before or at the same time as any significant change in canopy temperature.

Horseweed once again displayed results that differed greatly from the other species. Here, 63 out of 101 tests were deemed to be significant with 28 of those significant tests occurring before 60 hours after application. Horseweed continued to show differences even at the Bonferroni adjusted level of significance ($\alpha = 0.05/101$). At this p-level, 49 tests were significant with 15 tests occurring before 60 hours after application. This is an impactful finding because it indicates that significant canopy temperature differences in horseweed are detectable at a time period that is close to the time period in which visual symptoms may occur. The instances where susceptible horseweed exhibited significantly higher canopy temperatures than resistant horseweed is illustrated in Figure 2.9.

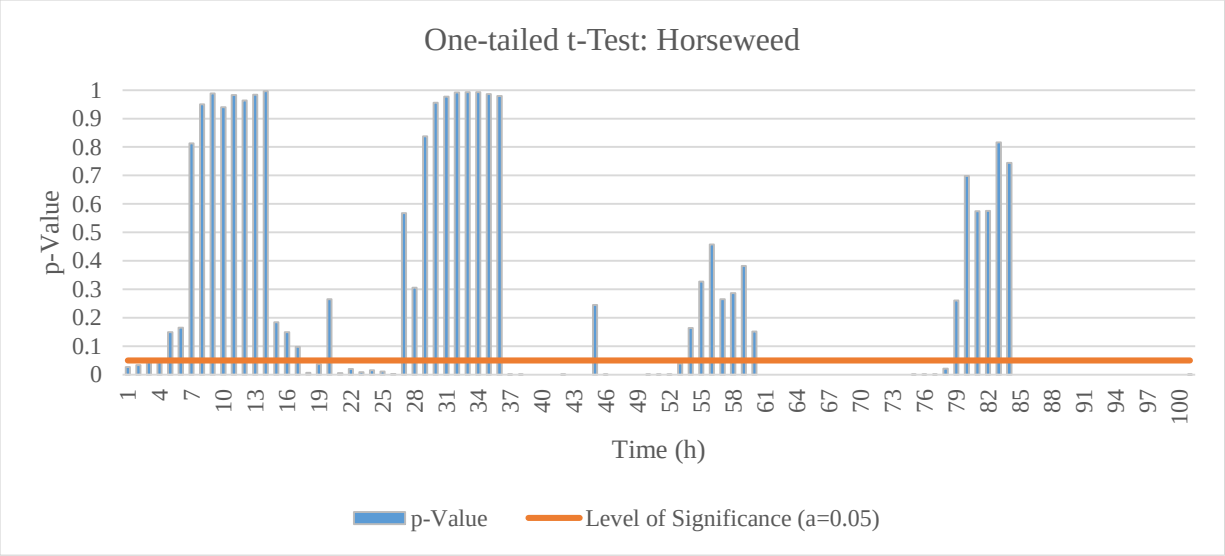

Figure 2.10. Results of One-tailed t-Test for Horseweed. Instances where bars do not pass the Level of Significance line indicate significantly higher glyphosate susceptible canopy temperatures

2.3.3. Stepwise Regression Analysis for Feature Selection

In 2019, the stepwise regression analysis that was conducted to select predictive variables (VAR_i) for classification resulted in standard errors of 0.464, 0.35, 0.253, 0.199, 0.129, and 0.086 for Palmer amaranth, red root pigweed, horseweed, waterhemp, ragweed, and kochia respectively. Each hour of data collected after application acted as the predictive variables for which the model would evaluate and select for optimal performance. The optimum number of variables were added to each model until the highest possible adjusted coefficient of determination (R^2) values was attained. R^2 values of 0.247, 0.526, 0.752, 0.846, 0.932, and 0.971 were recorded for Palmer amaranth, red root pigweed, horseweed, waterhemp, ragweed, and kochia respectively. The highest performing species, kochia, ragweed, and waterhemp, noticeably were the species that maintained consistently lower resistant biotype temperatures than susceptible in the original comparison. Based on the model performance, 15 predictive variables of VAR_{86}, VAR_{60}, VAR_{40}, VAR_{25}, VAR_{55}, VAR_{13}, VAR_{05}, VAR_{17}, VAR_{58}, VAR_{75},

and VAR_{27} were selected to establish the model for classification for glyphosate resistant kochia where VAR_{27} represents the canopy temperatures collected during the 27th interval of data collection with one image being collected every hour. Varying combinations of input variables occurred for each species.

Table 2.2. 2019 Experiment Summary of Stepwise Regression Model for Feature Selection

Model No.	Adjusted R^2						Std. Error of the Estimate					
	Palmer Amaranth	RRPW	Horseweed	Waterhemp	Ragweed	Kochia	Palmer Amaranth	RRPW	Horseweed	Waterhemp	Ragweed	Kochia
1.000	0.172	0.094	0.182	0.163	0.511	0.121	0.477	0.484	0.459	0.464	0.347	0.476
2.000	0.247	0.187	0.402	0.459	0.671	0.357	0.464	0.458	0.392	0.373	0.284	0.407
3.000		0.317	0.502	0.619	0.718	0.463		0.420	0.358	0.313	0.263	0.372
4.000		0.428	0.575	0.723	0.756	0.609		0.384	0.331	0.267	0.245	0.318
5.000		0.406	0.661	0.764	0.797	0.671		0.392	0.296	0.247	0.224	0.291
6.000		0.469	0.708	0.796	0.826	0.757		0.370	0.274	0.229	0.207	0.250
7.000		0.526	0.752	0.822	0.854	0.811		0.350	0.253	0.214	0.189	0.221
8.000				0.846	0.912	0.842				0.199	0.148	0.202
9.000					0.932	0.866					0.129	0.186
10.000						0.889						0.169
11.000						0.910						0.152
12.000						0.930						0.135
13.000						0.944						0.120
14.000						0.965						0.095
15.000						0.971						0.086

In 2020, the stepwise regression analysis resulted in standard errors 0.464, 0.404, 0.413, 0.366, and 0.23 for ragweed, waterhemp, kochia, Palmer amaranth, and horseweed, respectively. The optimum number of variables were added to each model until the highest possible adjusted coefficient of determination (R^2) values were attained. R^2 values of 0.146, 0.354, 0.32, 0.47, and 0.79 were attained for ragweed, waterhemp, kochia, Palmer Amaranth, and horseweed, respectively. Upon reviewing these values, it was determined that the model generated to select predictive variables (VAR_i) for horseweed was the only suitable model for further investigation. Each hour of data collected after application acted as the predictive variables for which the model would evaluate and select for optimal performance. The predictive variables selected for horseweed were VAR_{70}, VAR_{47}, VAR_{97}, VAR_{18}, VAR_{72}, VAR_{95}, VAR_{42} represents the dataset from the 70th hour of data collection and is the most statistically significant predictor for identifying glyphosate resistant horseweed. VAR_{47} served as the second most discriminative

predictor of glyphosate resistance in horseweed. After the inclusion of VAR_{47} in the model, the improvements to adjusted R^2 began to reduce significantly, suggesting that the inclusion of the other predictive variables do not contribute much to the model (Table 2.3.). Therefore, it can be assumed that it is unlikely that discrimination between glyphosate susceptible and glyphosate resistant horseweed plants will occur before 48 hours after application, which is the time period for visual symptoms to appear from glyphosate application (Monsanto, 2017).

Table 2.3. 2020 Experiment: Summary of Stepwise Regression Model for Feature Selection

Model No.	Adjusted R^2					Std. Error of the Estimate				
	Ragweed	Waterhemp	Kochia	Palmer Amaranth	Horseweed	Ragweed	Waterhemp	Kochia	Palmer Amaranth	Horseweed
1	0.1	0.086	0.053	0.079	0.583	0.477	0.480	0.487	0.482	0.325
2	0.146	0.152	0.123	0.254	0.636	0.464	0.463	0.469	0.434	0.303
3		0.197	0.197	0.285	0.678		0.450	0.449	0.425	0.285
4		0.236	0.234	0.357	0.723		0.439	0.438	0.403	0.265
5		0.225	0.271	0.414	0.751		0.442	0.428	0.385	0.251
6		0.249	0.329	0.452	0.77		0.435	0.410	0.372	0.241
7			0.32	0.47	0.782			0.413	0.366	0.235
8					0.793					0.229
9					0.79					0.23

2.3.4. Support Vector Machine Analysis

Despite the promising results from the stepwise regression in 2019, only poor to moderate classification accuracy was achieved using the support vector machine. Ragweed achieved the highest accuracy with 70%. However, it was also the smallest test set with only 10 plants being classified. The species with the highest R^2 from the stepwise regression, kochia, only managed classification accuracy of 50%. Waterhemp, horseweed, red root pigweed, and Palmer amaranth each achieved accuracies of 60%, 61.54%, 50% and 50% respectively. Classification results and performance metrics for the 2019 experiment are presented in Tables 2.4. and 2.5.

Table 2.4. Confusion Matrix of 2019 SVM Classification

2019		Predicted Value																	
		Kochia			Ragweed			Waterhemp			Horseweed			Red Root Pigweed			Palmer Amaranth		
		NO	YES	Total	NO	YES	Total	NO	YES	Total	NO	YES	Total	NO	YES	Total	NO	YES	Total
Actual Value	NO	3	7	10	3	2	5	2	5	7	4	3	7	2	5	7	6	1	7
	YES	3	7	10	1	4	5	1	7	8	2	4	6	2	5	7	6	1	7
Total		6	14	50.00%	4	6	70.00%	3	12	60.00%	6	7	61.54%	4	10	50%	12	2	50.00%

Table 2.5. Performance Summary of SVM Classification

Weed Species	Kochia	Ragweed	Waterhemp	Horseweed	Red Root Pigweed	Palmer Amaranth
Classification Accuracy%	50.00	70.00	60.00	61.54	50.00	50.00
Specificity	0.30	0.60	0.29	0.43	0.29	0.86
Sensitivity	0.70	0.80	0.88	0.67	0.71	0.14
Kappa Coefficient	0	0.54	0.59	0.49	0.56	0.19

In 2020, two positive classification results were recorded in the case of horseweed and waterhemp and can be found within Table 2.6 and 2.7. An accuracy result of 88.89% was achieved with a kappa score of 0.79 by using the SVM classifier. Waterhemp achieved an accuracy of 85% with a kappa score of 0.7. All other weed species failed to be reliably classified as accuracies of 44.44%, 50%, and 63.16% were achieved for kochia, ragweed, and Palmer amaranth respectively.

Table 2.6. Confusion Matrix of 2020 SVM Classification

2020		Predicted Value														
		Kochia			Ragweed			Waterhemp			Horseweed			Palmer Amaranth		
		NO	YES	Total	NO	YES	Total	NO	YES	Total	NO	YES	Total	NO	YES	Total
Actual Value	NO	6	11	10	3	4	3	8	2	7	10	0	10	2	7	9
	YES	4	6	10	3	4	4	1	9	8	2	6	8	0	10	10
Total		6	14	44.44%	11	10	50.00%	3	12	85.00%	12	6	88.89%	2	17	63.16%

Table 2.7. Performance Summary of 2020 SVM Classification

Weed Species	Kochia	Ragweed	Waterhemp	Horseweed	Palmer Amaranth
Classification Accuracy%	44.44	50	85	88.89	63.16
Specificity	0.22	0.42	0.80	0.20	0.22
Sensitivity	1	0.57	0.90	0.67	0.14
Kappa Coefficient	0.36	0	0.7	0.79	0.23

The attainment of better classification results in 2020 for waterhemp and horseweed is likely due to sampling performed to select plants with the most distinct differences in MoR. When applied to weeds that show varying MoR, this finding indicates that thermal data is not a reliable predictor to classify between glyphosate resistant and glyphosate susceptible weeds. However, it is seen that in cases where high distinction between resistance and susceptibility is present thermal data proves capable in achieving commendable results. The findings of Shirzadifar (2018) solely involved canopy temperatures taken from weed populations that showed polarizing differences in MoR, which is possibly a reason why results between studies differ significantly.

2.4. Conclusion

This study illustrated the debilitating effect of varying MoR on the accuracy of SVM classification of glyphosate resistant weeds using thermal data. The t-testing performed to test if the temperature of susceptible weeds was significantly greater than resistant weeds returned positive results only in horseweed where 63 out of 101 tests were deemed to have significantly higher susceptible temperatures than resistant temperatures. The SVM classifier results across 2019 and 2020 returned poor classification accuracy in all species except horseweed and waterhemp in 2020. This study, originally conducted with the goal of validating the previous method created by Shirzadifar (2018), shows that classification between glyphosate resistant and glyphosate susceptible weeds using thermal data is only possible in situations where there is great distinction between glyphosate susceptible weeds and herbicide resistant weeds that occurs within a 4-day period.

3. UAV-BASED THERMAL INFRARED AND MULTISPECTRAL IMAGING OF WEED CANOPIES FOR GLYPHOSATE RESISTANCE DETECTION

3.1. Introduction

The introduction of newer, higher resolution thermal imaging systems that are compatible with unmanned aerial vehicles (UAV) have boosted the practical use of thermography in agriculture. UAV thermal remote sensing applications include monitoring plant water stress, detection of diseases, and plant phenotyping (Sagan et al., 2019). Most of these applications are used to monitor crops, and the investigation of other types of vegetation within agricultural systems is low.

Weed control is a critical component to large-scale farming and the unexplored potential of thermal imagery using UAVs could boost the capabilities site-specific weed management technology. In most cases, thermal imagery brings value to producers through its ability to estimate a plant's stomatal conductance that may be suffering from water stress (Jones, 2018). Stomatal conductance is lessened in water stress times to mitigate transpiration and conserve water within the plant (Gimenez et al., 2013). The reduction in stomatal activity lowers the transpiration of water to be performed by the plant leaves, resulting in increased leaf temperature (Gonzalez-Dugo et al., 2019).

However, the inhibition of stomatal conductance is not only caused by water stress. The application of glyphosate to susceptible plants causes a reduced photosynthetic rate due the inhibition of stomatal conductance (Picoli et al., 2016). Glyphosate (N-phosphonomethyl-glycine) is one of the most commonly used herbicides in production agriculture. Developed in 1974, glyphosate is a non-selective herbicide that inhibits the enzyme enolpyruvyl shikimate-3-phosphate synthase (EPSPS) from developing amino acids that are required for protein synthesis

(Pollegioni et al., 2011). The highly effective herbicide quickly established widespread and repetitive use by crop producers, accelerating the evolution of resistance mechanisms within weeds (Christophers, 1999).

The work reported here sought to confirm previous findings that suggested that thermal imagery could be used to differentiate between glyphosate susceptible and glyphosate resistant weed populations based on canopy temperature (Shirzadifar, 2018). The original study was performed using thermal imagery on an extremely small spatial scale where each image used for classification only covered 1.6 m^2. This study was designed to investigate the potential of thermal data on a larger area than the original study and compares thermal imagery performance to additional multispectral sensors.

3.2. Materials and Methods

3.2.1. Study Site and Experimental Setup

The experiment was conducted at two locations, one being the NDSU Agronomy Seed Farm in Casselton, North Dakota, USA while the other was conducted at the NDSU Research and Extension Center in Carrington, North Dakota, USA. Each location contained a plot measuring approximately 33 m in length and 3.5 m in width (115 m^2). Data collections were performed from the middle to end of August 2020.

At the Casselton location (Figure 3.1.), a combination of Roundup Ready 2 Xtend and ND Stutsman (NDSU) conventional soybeans were planted in alternating fashion in 4 rows with 30-inch row spacing. A center-pivot irrigation system was not available at this site so water was provided to the weed plants using a truck-mounted water tank. At this location, the soil series was predominantly Kindred-Bearden silty clay loams that are somewhat poorly drained and nonsaline (Soil Survey Staff, 2005). Buckets of soil were collected at the location and brought to

the Agricultural Experiment Station Greenhouse at the NDSU campus in Fargo, ND to be autoclaved to sterilize the soil of weed seeds and microbiological inhabitants. Once the autoclave process was complete, the soil was used to germinate the weed populations in greenhouse conditions at another location on campus. A total of 60 kochia plants, 60 waterhemp plants, 60 red root pigweed plants, and 30 ragweed plants were successfully grown and transplanted to the field. To increase plant population, a selection of naturally occurring ragweed plants was transplanted from site location and introduced to the plot, resulting in a total number of 59 ragweed plants. The weed populations were comprised equally of 2 different biotypes, one being selected for glyphosate resistance and the other for glyphosate susceptibility. Plants were organized in a randomized complete block design based on their believed resistance status and planted in between the soybean rows with one species occupying a single row at a time. When the weeds were approximately 12-15cm tall, 28 oz/a of Roundup Powermax (48.7% glyphosate) with Class Act NG at 2% v/v was applied to the plot in an attempt to induce symptomology on the susceptible biotypes. Post-experiment visual evaluations were performed 14 days after application (14DAA). The evaluations showed that varying degrees of glyphosate resistance occurred in the species. The magnitudes of resistance observed at the Casselton location are summarized within Table 3.1. where weeds are grouped based on their resistance status.

Table 3.1. Casselton Plant Survival Evaluation (14DAA)

Species Rating	Magnitude of Resistance						# Observed	
	0	1	2	3	4	5	Susc.	Res.
Kochia	21	12	2	10	6	6	35	22
Ragweed	42	10	0	0	10	5	52	7
Waterhemp	0	0	0	0	15	45	0	60
Red Root Pigweed	52	8	0	0	0	0	60	0

Magnitude of Resistance: 0=Dead Plants 5=Alive Plants with no Symptoms

Figure 3.1. RGB mosaic of Casselton field experiment location

At the Carrington location (Figure 3.2a), five rows of Roundup Ready 2 Xtend (Bayer, Whippany, NJ) Soybeans (Glycine Max) were planted with 30-inch row spacing. A center pivot irrigation system at this location was utilized to provide a constant water source for the plot. The soil series present at this location is predominantly Fram-Wyard (G211A) loams which are somewhat poorly drained and slightly saline (Soil Survey Staff, 2014). Buckets of soil were also collected at this location and brought to the Agricultural Experiment Station Greenhouse at NDSU in Fargo, ND to be autoclaved in order to sterilize the soil of weed seeds or microbiological inhabitants. The soil was then returned to a greenhouse located at the Carrington location where weed populations were grown in 3-in diameter pots. A total of 60 kochia plants, 60 waterhemp plants, 60 red root pigweed plants and 30 ragweed plants were successfully grown and then transplanted to the field plot in randomized fashion (Figure 3.2b). When the weeds were approximately 12-15cm tall, 28 oz/a of Roundup Powermax (48.7% glyphosate) with Class Act NG at 2% v/v was applied to the plot in an attempt to induce symptomology on the susceptible biotypes. Both the Casselton and Carrington locations shared the same source of seeds so the varying degrees of resistance observed at Casselton were seen at Carrington. However, the herbicide's efficacy was noticeably less at the Carrington site, as symptomology was seen as early as 2DAA at the Casselton site but not seen until 6DAA at the Carrington site. The rates of susceptibility observed at the Carrington location are summarized within Table 3.2.

Table 3.2. Carrington Plant Survival Evaluation (14DAA)

Species Rating	Magnitude of Resistance						# Observed	
	0	1	2	3	4	5	Susc.	Res.
Kochia	1	7	17	7	9	19	25	35
Ragweed	2	3	3	7	10	5	8	22
Waterhemp	0	0	0	0	18	42	0	60
Red Root Pigweed	40	20	0	0	0	0	60	0

Magnitude of Resistance: 0=Dead Plants 5=Alive Plants with no Symptoms

a)

b)

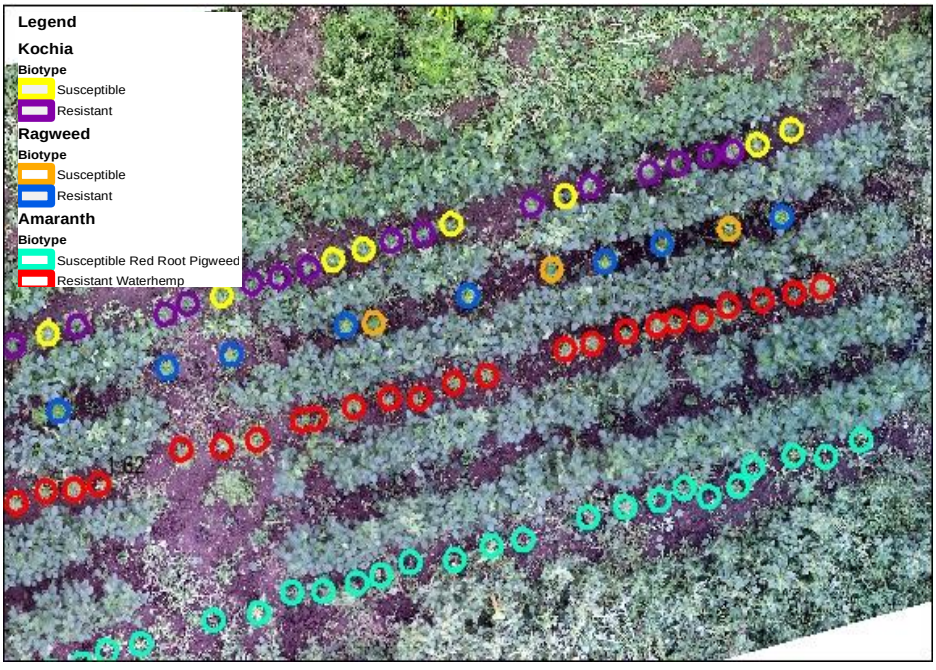

Figure 3.2. a) Mosaic of Carrington Field Experiment Location b) Randomization scheme used at both locations

3.2.2. UAV Equipment and Flight Parameters

Image data for the plots were performed using a Zenmuse XT2 RGB/Thermal camera (DJI Technology Co., Ltd., Shenzhen, China) and a Micasense Red-Edge MX Dual Camera System (Micasense, Seattle, USA). The Zenmuse XT2 provided both RGB and thermal image data, but only the thermal image data was used for testing. The Red-Edge MX Dual Camera system provided ten bands of spectral data. Imagers on the dual camera provided a selection of imagery around the blue, green, red, red-edge and near-infrared (NIR) wavelengths. Both systems were mounted simultaneously on a DJI M600 Pro UAV (DJI Technology Co., Ltd., Shenzhen, China).

Due to restrictions with the flight planning software, simultaneous image capture for both systems could not be performed at an altitude less than 25m. Therefore, an 8m manual flight was conducted solely using the Zenmuse XT2 while separate automated flights were performed at 10m while capturing imagery with the Red-Edge MX Dual Camera system. Automated flights for the Red-Edge MX Dual Camera were planned and performed using Pix4D capture mobile app on iOS. This approach allowed for greater spatial resolution with the thermal camera, as the XT2 has a lower resolution than the Red-Edge MX Dual Camera system. Image data captured with the Red-Edge MX Dual Camera was calibrated using a provided reflectance panel from Micasense to transform raw pixel values to absolute reflectance.

Imagery was captured at 4 and 6 DAA at both locations. An extra flight was performed 8 DAA at Casselton. Weather conditions at the Carrington during the 8DAA time period prevented a flight from being performed. Georeferencing for the imagery was performed by the inclusion of ground control points (GCPs). The GCPs consisted of white 5-gallon bucket lids with colored stakes driven through the center of them to provide a distinct center point. A Trimble Geo-7x

Handheld Data Collector and Zephyr 3 for GIS GNSS antenna (Trimble Geospatial, Westminster, Sunnyvale, USA) was then used to capture the GCP locations with 2cm accuracy. Five GCPs were placed at each site with four points at the field corners and one point at the center. In cases where thermal imagery was being captured, cold water was placed over the bucket lids to be easily visible in the imagery. In addition to GCP collection, GPS data was collected from the approximate centroid of each plant location for later use in GIS mapping software.

Imagery was stitched into reflectance ortho-mosaics using Pix4Dmapper Version 4.5.6 (Pix4D, Prilly, Switzerland). Near-Infrared and red wavelength imagery from the Red-Edge MX Dual Camera system were used to generate an additional NDVI mosaic. Approximately 150-200 image captures were taken per flight and used for mosaic generation. Ground control point data from the Trimble GPS was incorporated in the processing procedure to grant spatial accuracy as high as 2cm.

A complete list of flight operations and equipment parameters is summarized in Table 3.3. and the weather conditions for each flight is listed in Table 3.4.

Table 3.3. UAS Flight Operations Summary

Equipment and Parameters	Camera Type	
	Multispectral	Thermal
UAS Model	DJI M600	DJI M600
Sensor	Micasense Red-Edge Dual Camera	Zenmuse XT2 Thermal Camera
Pixel Resolution	1280 x 960	640x512
Focal Length	5.4mm	25mm
Channels	444, 475, 531, 560, 650, 668, 705, 717,740, 842 (nm)	7.5-13.5 (μm)
Average altitude	10m	8m
Ground Spatial Distance (GSD)	0.71cm	1.03cm
Forward overlap	75%	+80%
Side overlap	75%	+80%
FOV	47.2° HFOV	25° HFOV

Table 3.4. Weather Conditions During Data Collection

Site	Days After Application	Collection Time	Air Temp (°C)	Relative Humididty (%)	Solar Radiation (Lys)
Casselton	4	10:30-11:30	21.77	74	14.5
	6	10:30-11:30	23.31	55	61
	8	10:30-11:30	22.68	77.5	37.5
Carrington	4	10:30-11:30	23.73	65	52
	6	10:30-11:30	22.39	80	33

3.2.3. Extraction of Vegetation and Development of Classification Zones

Once the images gathered from the experiments were processed into mosaics, they were visualized using ArcGIS Pro (ESRI, Redlands, CA). The plant GPS data was then overlaid as point shapefiles. The Buffer tool in ArcGIS Pro was then used to create 12cm buffer shapefiles around the centroid of the pots. Buffers were inspected for accurate placement in the imagery and corrected if necessary. Buffers were then selected and separated into their own respective species using the Clip tool. The visual survival evaluation results were then added to the shapefile attribute table to further separate the buffers into resistant and susceptible biotypes within each species.

The buffers were then used to extract 12cm diameter raster information from each image datasets, vastly reducing the amount of imagery so that only the plant locations would be subjected to further processes. This approach, however, still left a mixture of soil and vegetation within the buffers. To increase the extraction accuracy even further, the Extract by Attributes tool was used to extract pixels from the buffers that had an NDVI value greater than 0.4. This action removed the soil from the buffers so that only vegetation would be displayed. The NDVI output was then used to remove soil pixels from the thermal and multispectral rasters using the Extract by Mask tool. The complete extraction process is illustrated in Figure 3.3.

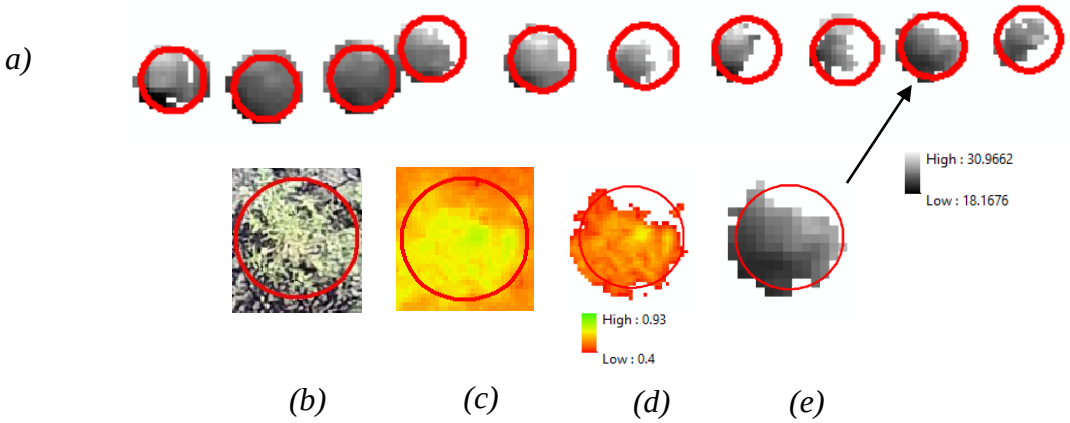

Figure 3.3. Result of extracted thermal data from Kochia at the Casselton location. a) final product after NDVI extraction b) RGB image of kochia for reference c) NDVI of kochia prior to 0.4 pixel value extraction d) NDVI mask containing pixels that score over 0.4 e) NDVI mask applied to thermal data (°C)

Sets of buffers were created for each species and separated into classes based upon their resistance status. In addition to thermal extraction from the Zenmuse XT2, extractions of NDVI and a 3-band composite image from the Red-Edge MX Dual Camera system were also made to serve as comparisons. By using the Spectral Profile tool within ArcGIS, the reflectance of glyphosate resistant vegetation and glyphosate susceptible vegetation were compared at each of the ten bands provided by the Red-Edge MX Dual Camera system (Figure 3.4a). Bands 5,7, and 9 from the Red-Edge MX Dual Camera (842nm, 705nm, & 740nm, respectively) were selected because large differences in reflectance were found at these wavelengths between glyphosate resistant vegetation and glyphosate susceptible vegetation. Bands 5, 7, & 9 were subsequently used to create a composite image that served as a third data source for classification attempts (Figure 3.4b).

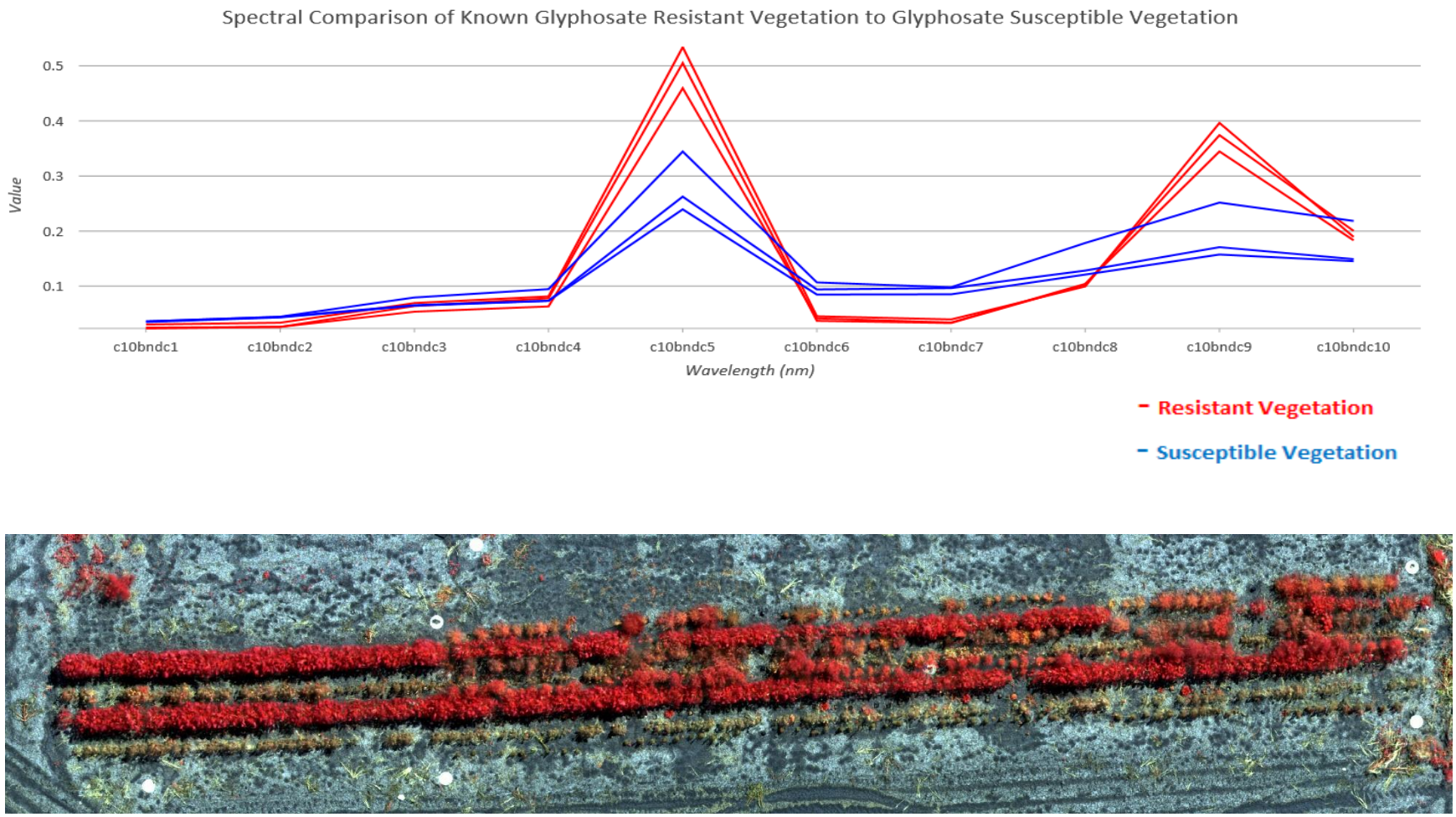

Figure 3.4. a) Spectral profile illustrating differences seen at band 5, 7, and 9 between glyphosate resistant vegetation and glyphosate susceptible vegetation b) Image of Casselton site 8DAA using band combination 5,7, & 9 (842nm, 705nm, and 740nm) from Red-Edge MX Dual Camera

3.2.4. Raster Classification of Glyphosate Resistant and Glyphosate Susceptible Weeds

Once the buffered and extracted datasets were created, they were then classified using the Image Classification Wizard in ArcGIS Pro. Training zones were created over the plant locations using the buffer shapefiles that were separated based upon resistance status and then conjoined to create a training template containing two classes: glyphosate susceptible vegetation and the other being glyphosate resistant vegetation. Each classification was performed on each species independently from one another except in the case of waterhemp and red root pigweed. The MoR of resistance did not have any variation within the respective species as the waterhemp population was determined to be completely resistant to the glyphosate application while the red root pigweed population was determined to be completely susceptible to the glyphosate application.

That being said, waterhemp and red root pigweed both are in the same genus of herbaceous plants (*Amaranthus L.)* commonly referred to as pigweeds (NRCS, 2020). Rather than sacrificing their presence in the study because of their unfavorable resistance statuses, the two species were paired together because of their close relation to each other. The waterhemp served as a glyphosate resistant population and red root pigweed served as a susceptible population. This approach sacrificed the randomization schemes seen in kochia and ragweed, making thermal classification results unreliable due to spatial temperature differences of areas within the scene. NDVI and band combination 579 however, still is somewhat reliable as spectral reflectance of vegetation is more consistent despite its location within the scene as all plants received approximately the same amount of sunlight. In addition to weed classifications, a classification was made between the Round-up Ready soybean and conventional Stutsman

soybean at Casselton 8DAA to see if thermal classification performance can be greatly improved when dealing with known opposing MoR ratings.

Pixel based image analysis was used to classify the biotypes. Three classification methods were used to classify each species raster data set for each of the three days. Data was collected to compare classification accuracy between the imaging systems and classification methods. Maximum likelihood (ML), random trees (RT), and support vector machine (SVM) were the three classification methods used.

The support vector machine classification method utilized only a subset of the pixels included in the raster datasets to act as training data for the classifier. The maximum samples per class was set to the default value of 500 pixels for each class. The random trees classifier similarly used only a subset of pixels but with a default value of 1000 pixels. The maximum likelihood classifier was also used with its default settings.

3.2.5. Accuracy Assessments of Thermal, NDVI, and Band 579 Classifications

To test the accuracy of the generated classifications, the Create Accuracy Assessment within ArcGIS Pro was used to digitize ground truth points within each classification raster's extents. Pixels that belonged to plant that was determined to be glyphosate susceptible within the survival evaluation were assigned the value of 0, while pixels that belonged to a glyphosate resistant plant were assigned a value of 1. Approximately 1000 points were used for every species. The points were then updated by recording the values of the point locations observed in the classification raster, which provided a shapefile with both ground truth and classification fields with raster values ranging from 0-1. The Compute Confusion Matrix tool was then used to observe the accuracy and kappa coefficient of each classification attempt.

3.3. Results and Discussion

Overall, classification performance was somewhat poor within kochia and ragweed observations. However, improvements in classification accuracy were observed across the total data collection period for each site with band combination 5,7, & 9 from the Red-Edge MX Dual Camera providing the highest accuracy and kappa coefficient results. This effect is expected, as the herbicide is provided more time to induce symptomology and gradually desiccate the susceptible population due to the inhibition of stomatal conductance often observed with glyphosate application (Picoli et al., 2017).

3.3.1. Classification of Glyphosate Resistant Kochia

The Kappa coefficient values for kochia at 4DAA suggested only slight agreement at best between the classification and ground truth fields of band combination 579 at the Casselton location (Table 3.5). The random trees classifier performed the best at 4DAA with an accuracy of 62.9%. At 6DAA, performance slightly improved in all band combinations. Band 579 at the Casselton location with the random trees classifier once again achieved the highest classification accuracy and kappa coefficient results at this time period with values of 74% and 0.471 respectively. The 8DAA kochia classification at Casselton once again improved in performance. The maximum likelihood classifier provided the highest performing result out of all classification attempts with an accuracy of 75.2% and a kappa coefficient of 0.487.

Thermal classifications for kochia were noticeably the lowest performing of the three tested band options. The highest performing thermal classification, which used the random trees method at 8DAA was outperformed by all NDVI and band combination 579 classifications. This finding suggests that thermal canopy temperature data is not a reliable predictor of glyphosate resistance in kochia and that multispectral data should be further investigated.

Table 3.5. Carrington Kochia Classification Performance Summary

4DAA				6DAA			
Band Selection	Method	Accuracy	Kappa	Band Selection	Method	Accuracy	Kappa
Thermal	ML	0.591	0.089	Thermal	ML	0.576	0.151
	RT	0.507	0.015		RT	0.589	0.162
	SVM	0.542	0.102		SVM	0.587	0.177
NDVI	ML	0.572	0.04	NDVI	ML	0.637	0.286
	RT	0.572	0.04		RT	0.606	0.115
	SVM	0.566	0.07		SVM	0.623	0.257
Band 579	ML	0.584	0.167	Band 579	ML	0.673	0.3
	RT	0.591	0.134		RT	0.727	0.453
	SVM	0.584	0.148		SVM	0.667	0.334

Table 3.6. Casselton Kochia Classification Performance Summary

4DAA				6DAA				8DAA			
Band Selection	Method	Accuracy	Kappa	Band Selection	Method	Accuracy	Kappa	Band Selection	Method	Accuracy	Kappa
Thermal	ML	0.576	0.133	Thermal	ML	0.577	0.161	Thermal	ML	0.579	0.17
	RT	0.548	0.087		RT	0.58	0.163		RT	0.622	0.22
	SVM	0.497	-0.004		SVM	0.563	0.126		SVM	0.602	0.181
NDVI	ML	0.559	0.011	NDVI	ML	0.638	0.276	NDVI	ML	0.654	0.283
	RT	0.605	0.179		RT	0.667	0.317		RT	0.724	0.401
	SVM	0.588	0.177		SVM	0.666	0.314		SVM	0.726	0.388
Band 579	ML	0.609	0.224	Band 579	ML	0.691	0.385	Band 579	ML	0.752	0.487
	RT	0.629	0.258		RT	0.74	0.471		RT	0.742	0.463
	SVM	0.577	0.19		SVM	0.706	0.372		SVM	0.748	0.482

3.3.2. Classification of Glyphosate Resistant Ragweed

Generally, poor classification performance was seen in ragweed as well. Only 8 ragweed plants at the Carrington site succumbed to the glyphosate application and 22 survived. The weeds showed varying levels of resistance, which likely also reduced the classifier's capability to distinguish between the two biotypes. Contrary to the Casselton site, a large number of susceptible ragweed dominated the Casselton site, leaving only 7 resistant weeds. The natural population of ragweed that was introduced to the study to increase population sizes was determined to be part of the cause for such varying numbers, but it can also be noted that the glyphosate symptomology appeared much sooner and more severely than at Carrington. Despite difficulties in the 4DAA and 6DAA data collections, a commendable classification was made by the NDVI 8DAA in Casselton, where the random trees classifier attained an accuracy of 87.2%

with a kappa of 0.413. In order to determine the effectiveness of thermal data to identify glyphosate resistance in ragweed, it is necessary that more data must be gathered

Table 3.7. Carrington Ragweed Classification Performance Summary

4DAA				6DAA			
Band Selection	Method	Accuracy	Kappa	Band Selection	Method	Accuracy	Kappa
Thermal	ML	0.591	0.089	Thermal	ML	0.477	0.045
	RT	0.507	0.015		RT	0.643	0.25
	SVM	0.542	0.102		SVM	0.484	0.06
NDVI	ML	0.32	0.03	NDVI	ML	0.329	0.031
	RT	0.483	0.056		RT	0.574	0.127
	SVM	0.441	0.022		SVM	0.565	0.119
Band 579	ML	0.428	0.067	Band 579	ML	0.29	0.036
	RT	0.618	0.25		RT	0.656	0.3
	SVM	0.564	0.191		SVM	0.633	0.263

Table 3.8. Casselton Ragweed Classification Performance Summary

4DAA				6DAA				8DAA			
Band Selection	Method	Accuracy	Kappa	Band Selection	Method	Accuracy	Kappa	Band Selection	Method	Accuracy	Kappa
Thermal	ML	0.582	-0.057	Thermal	ML	0.622	-0.046	Thermal	ML	0.43	0.071
	RT	0.568	0.13		RT	0.514	0.051		RT	0.627	0.119
	SVM	0.592	0.052		SVM	0.442	0.02		SVM	0.562	0.055
NDVI	ML	0.704	-0.087	NDVI	ML	0.642	0.099	NDVI	ML	0.728	0.179
	RT	0.562	0.05		RT	0.643	0.174		RT	0.778	0.27
	SVM	0.54	0.066		SVM	0.689	0.124		SVM	0.872	0.413
Band 579	ML	0.552	0.096	Band 579	ML	0.711	0.157	Band 579	ML	0.761	0.246
	RT	0.635	0.113		RT	0.767	0.37		RT	0.769	0.303
	SVM	0.536	0.071		SVM	0.755	0.231		SVM	0.767	0.278

3.3.3. Classification of Glyphosate Resistant Amaranth Results

The amaranth dataset (composed of resistant waterhemp and susceptible red root pigweed) exhibited much higher accuracy and kappa scores for thermal classifications, although these values are likely inflated. The Carrington site's thermal classifications likely received such high accuracy and kappa scores solely because of the two species' spatial location within the scene. The resistant waterhemp population filled the interior of a soybean row with dense vegetation that was near canopy closure. The soybean canopy provided shelter for the waterhemp, while the red root pigweed was positioned on the outside of a soybean row, it was directly exposed to sunlight. The presence of shadows over vegetation provide a cooling effect

to the waterhemp plant areas. Shaded areas receive diffused solar radiation compared to areas in direct sunlight, leading to a significant temperature differential (Renhua, et al., 2001). In addition to the difference in spatial location, the polarizing differences in MoR that were observed could also further cause an easily detectable temperature differential between the two species, where the resistant waterhemp canopies showed cooler temperatures than the susceptible red root pigweed canopies.

It is possible that the difference in spatial location was not as much of a factor at the Casselton location as sunlight exposure was approximately the same for both species. Due to the north facing orientation of the plot, sunlight was provided parallel to the soybean rows at the time of data collection rather than across dense soybean rows as in Carrington. This reasoning could offer explanation as to why the Carrington location received higher accuracy results than Casselton. Regardless, this approach illustrates the powerful impact of spatial variability of temperature on classification accuracy using thermal sensors. Weeds that were placed only a few feet away from each other exhibited significantly different canopy temperatures because of different levels of exposure to sunlight. While the spatial variability and presence of crops could potentially impact the thermal readings, reflectance values from a multispectral sensor are less susceptible to the same degree of contamination as sunlight reflectance is the value being recorded and not temperature. Therefore, the superior performance shown by the multispectral sensors serves as another indicator that thermal classifications are not reliable. The results of the Amaranth classifications are summarized in Tables 3.9. and 3.10.

Table 3.9. Carrington Amaranth Classification Performance Summary

4DAA				6DAA			
Band Selection	Method	Accuracy	Kappa	Band Selection	Method	Accuracy	Kappa
Thermal	ML	0.778	0.554	Thermal	ML	0.707	0.406
	RT	0.793	0.587		RT	0.956	0.912
	SVM	0.796	0.592		SVM	0.92	0.84
NDVI	ML	0.769	0.535	NDVI	ML	0.865	0.729
	RT	0.727	0.454		RT	0.869	0.737
	SVM	0.779	0.558		SVM	0.861	0.722
Band 579	ML	0.778	0.554	Band 579	ML	0.911	0.822
	RT	0.796	0.592		RT	0.836	0.671
	SVM	0.793	0.587		SVM	0.907	0.813

Table 3.10. Casselton Amaranth Classification Performance Summary

4DAA				6DAA				8DAA			
Band Selection	Method	Accuracy	Kappa	Band Selection	Method	Accuracy	Kappa	Band Selection	Method	Accuracy	Kappa
Thermal	ML	0.775	0.457	Thermal	ML	0.783	0.489	Thermal	ML	0.7	0.274
	RT	0.721	0.389		RT	0.745	0.43		RT	0.678	0.177
	SVM	0.79	0.474		SVM	0.796	0.499		SVM	0.651	0.278
NDVI	ML	0.971	0.935	NDVI	ML	0.969	0.939	NDVI	ML	0.923	0.8
	RT	0.967	0.926		RT	0.976	0.944		RT	0.935	0.81
	SVM	0.972	0.936		SVM	0.98	0.954		SVM	0.919	0.796
Band 579	ML	0.977	0.947	Band 579	ML	0.942	0.856	Band 579	ML	0.935	0.82
	RT	0.967	0.926		RT	0.988	0.972		RT	0.927	0.81
	SVM	0.97	0.932		SVM	0.986	0.968		SVM	0.919	0.796

3.3.4. Soybean Observation Results

A final attempt at distinguishing between glyphosate resistant vegetation and glyphosate susceptible vegetation was made using the conventional Stutsman soybeans and Xtend2 Round-Up Ready soybeans at the Casselton location. The observation made to investigate the classification accuracy attained when dealing with vegetation with known opposing MoR found that multispectral data generally shows better potential for classification between glyphosate resistant and glyphosate susceptible vegetation. However, thermal classifications showed higher performance at 4DAA than NDVI or the Band 579 (Table 3.11.). This finding was unexpected, as thermal classifications for any of the weed species did not exhibit similar performance levels at this time interval. This outlier in classification performance could result from incorporating highly glyphosate susceptible Stutsman soybeans and glyphosate tolerant Xtend 2 Round Up

Ready soybeans. This degree of difference in resistance status is highly unlikely in natural populations of weeds as resistance to glyphosate is generally conferred at a low MoR (2 or 3) which is why high doses of herbicide are recommended to impede glyphosate resistance (Sammons et al., 2007). An additional suggestion for the increased performance is that the increased amount of vegetation area was able to be captured more effectively with the lower resolution thermal camera, thus encouraging segregation between classes. The Zenmuse XT2 thermal camera provided 1.03 cm/pixel spatial resolution (Table 3.3.). The average leaf diameter of the soybeans was 7cm. The largest weed average leaf diameter belonged to waterhemp and was only 2-3cm. Therefore, it is possible that there were many more reliable thermal signatures captured off of soybean canopies than weed canopies. Reliable soybean canopy temperature extraction has proven to be possible with spatial resolutions as high as 0.8 m when investigating stomatal closure due to drought conditions (Crusiol et al., 2020).

Table 3.11. Casselton Soybean Classification Performance Summary

4DAA				6DAA				8DAA			
Band Selection	Method	Accuracy	Kappa	Band Selection	Method	Accuracy	Kappa	Band Selection	Method	Accuracy	Kappa
Thermal	ML	0.942	0.88	Thermal	ML	0.82	0.62	Thermal	ML	0.886	0.76
	RT	0.918	0.83		RT	0.77	0.52		RT	0.908	0.81
	SVM	0.936	0.87		SVM	0.79	0.56		SVM	0.889	0.77
NDVI	ML	0.794	0.55	NDVI	ML	0.944	0.89	NDVI	ML	0.977	0.95
	RT	0.71	0.41		RT	0.935	0.86		RT	0.981	0.96
	SVM	0.742	0.45		SVM	0.941	0.88		SVM	0.983	0.96
Band 579	ML	0.824	0.636	Band 579	ML	0.953	0.9	Band 579	ML	0.987	0.972
	RT	0.82	0.64		RT	0.907	0.808		RT	0.978	0.954
	SVM	0.824	0.65		SVM	0.963	0.922		SVM	0.981	0.959

3.4. Conclusion

This study's findings firmly suggest that using thermal imagery data as a predictor for glyphosate resistance within weed populations in field conditions is unreliable and susceptible to environmental variability. While technological advancements have provided increased resolutions in thermal systems, it was observed that higher resolution is needed to make investigations at the individual plant level using thermal data more scalable. NDVI and a

composite image comprised of 842nm, 705nm, and 740nm imagery managed to provide better classification results than thermal in most cases, but classifications performed within a single species to segregate glyphosate resistant and glyphosate susceptible biotypes of weeds still were not definitive. The high classification accuracy obtained in the cases of amaranth plants and soybeans supports the notion that extreme differences in MoR are necessary for any reliable attempt to identify glyphosate resistant vegetation regardless of using multispectral or thermal data as a predictor.

4. FUTURE RESEARCH

In the greenhouse, the use of only 10 pixel values from the weed canopies expresses a drastic need for an improved extraction method across large time periods. The optimal method to do this would be to find a way to generate an NDVI or RGB mask that aligns with the thermal data so that a mask image could be gathered with every thermal image. Using cool water to create a thermal mask image is possible, but it is only useful for a single image capture interval and then must be reapplied for future captures. The field research performed in this thesis was performed on weeds with varying magnitudes of glyphosate resistance. Future studies focused on an open rangeland setting where there is an establishment of natural weed populations that is not interrupted by the presence of crop rows may reduce the amount of variability in canopy temperature caused by sunlight blockage from other objects in the scene.

REFERENCES

Christophers, M. (1999). Genetic Aspects of Herbicide-Resistant Weed Management. *Weed Tech.*, 13(3), 647-652.

Chatham, L., Bradley, K. Kruger, G. Martin, J. Owen, M. Peterson, D. Mithila., J. Tranel, P. (2015). A Multisate Study of the Association Between Glyphosate Resistance and EPSPS Gene Amplification in Waterhemp (Amaranthus tuberculatus). Weed Science. 63 (3), 569-577.

Crusiol, L. Nanni, M. Furlanetto, R. Sibaldelli, R. Cezar, E. Mertz-Henning, L. Nepomuceno, A. Neumaier, N. Farias, J. (2019). UAV-based thermal imaging in the assessment of water status of soybean plants. *Intl. Journ. Rem. Sen.* 41(9), 3243-3265.

Delye, C. Duhoux, Pernin F., Riggins C., and Tranel, P. (2015). Molecular Mechanisms of Herbicide Resistance. *Weed Science*. 63, 91-115.

Dyrmann, M. Mortensen, A. Midtiby, S. Jorgenson, R. (2016). Pixel-wise Classification of Weeds in Crops in Images by using a Fully Convolutional Neural Network." *Proceedings of the CIG-AgEng Conference (2016).*

Evans, J.A. et. Al. (2015). Managing the evolution of herbicide resistance. *Pest Mgmt. Science.* 72(1), 74-80.

ESRI. (2020). Train Random Trees Classifier. Environmental Systems Research Institute. Retrieved from https://desktop.arcgis.com/en/arcmap/latest/tools/spatial-analyst-toolbox/train-random-trees-classifier.htm

Feng, P. C. C., M. Tran, T. Chiu, R. Sammons, G. Heck, and C. Cajacob. (2004). Investigations into glyphosate-resistant horseweed (Conyza canadensis): re-tention, uptake, translocation and metabolism. *Weed Science*. 52, 498-593

Fernandez, C. Leblon, B. Haddadi, A. Wang, K. Wang, J. (2020). Potato Late Blight Detection at the Leaf and Canopy Levels Based In the Red and Red-Edge Spectral Regions. *Environmental Mapping Using Remote Sensing.* 12(8), 1292.

Furey, T. Cristianini, N. Duffy, N. Bednarski, D., Schummer, M., Haussler, D. (2000). Support vector machine classification and validation of cancer tissue samples using microarray expression data. *Bioinformatics,* 16(10), 906-914.

Gaines, T.A., Zhang, W., Wang, D., Bukun, B., Chisholm, S.T., Shaner, D.L., Nissen, S.J.,Patzoldt, W.L., Tranel, P.J., Culpepper, A.S., Grey, T.L., Webster, T.M., Vencill, W.K.,Sammons, R.D., Jiang, J.M., Preston, C., Leach, J.E., Westra, P., (2010). Gene amplification confers glyphosate resistance in Amaranthus palmeri. *Proc. Natl. Acad. Sci.* U. S.A. 107, 1029-1034

Ge, X., d'Avignon D., Ackerman, J., Sammons, R. (2010). Rapidvacuolar sequestration: the horseweed glyphosate resistance mechanism. *Pest Management*. Sci 66, 345–348

Gomes, M.P., Manac'h, L., Sarah, G., Hénault-Ethier, L., Labrecque, M., Lucotte, M., Juneau, P. (2017). Glyphosate-dependent inhibition of photosynthesis in willow. *Frontiers in plant science*, 8, 207.

Gonzalez-Dugo, V.; Goldhamer, D.; Zarco-Tejada, P.J.; Fereres, E. (2015). Improving the precision of irrigation in a pistachio farm using an unmanned airborne thermal system. *Irrig. Sci*. 33, 43–52.

Gonzalez-Dugo V., Lopez-Lopez M., Espadafor M., Orgaz, F., Testi, L., Zarco, P, Lorite, I. Fereres, E. (2019). Transpiration from canopy temperature: Implications for the assessment of crop yield in almond orchards. *European J. of Agron*. 105, 78-85.

Guo J., Tian G., Zhou Y., Wang M., Ling N., Shen Q. and Guo S. (2016). Evaluation of the grain yield and nitrogen nutrient status of wheat (Triticum aestivum L.) using thermal imaging. *Field Crop Res*., 196, 463-472

Hartzler, B. 2017. The cost of herbicide resistance. Iowa State Extension: Integrated Crop Management. Retrieved from https://crops.extension.iastate.edu/blog/bob-hartzler/cost-herbicide-resistance

Jones, H., Serraj, B., Loveys, L. Xiong, A., Wheaton, Price, A. (2009). Thermal infrared imaging of crop canopies for the remote diagnosis and quantification of plant responses to water stress in the field. *Func. Plant. Bio*. 36, 978-989.

Jones, H. (2018). Thermal Imaging and Infrared Sensing in Plant Ecophysiology. In A. Sanchez-Moreiras and M. Reigosa (Eds.) *Advances in Plant Ecophysiology Techniques.* 135-151

Livingston, M., Fernandez-Cornejo, J., Unger, J., Osteen, C., Schimmelpfennig, D., Park, T., Lambert, D.M. (2015). The economics of glyphosate resistance management in corn and soybean production. Economic Research Service. USDA.

Kumar, V. Jha, P. (2015). Growth and Reproduction of Glyphosate-Resistant and Susceptible Populations of Kochia scoparia. *PLoS ONE*. 10(11).

Liu, J. Chen, P. 2018. Estimating Wheat Coverage Using Multispectral Images Collected by Unmanned Aerial Vehicles and a New Sensor. IEEE.

Mangus, D., Sharda, A., Zhang, N. (2016). Development and evaluation of thermal infrared imaging system for high spatial and temporal resolution crop water stress monitoring of corn within a greenhouse. Computers and Electronics in Agriculture, 121, 149-159.

MicaSense. (2017). The Science Behind MicaSense. Retrieved from https://micasense.com/the-science-behind-micasense/

Monsanto Company. (2017). Roundup PowerMax II Herbicide: Complete Directions for Use. St. Louis, MO.

Pollegioni, L., Schonbrunn, E., Siehl, D. (2011). Molecular basis of glyphosate resistance–different approaches through protein engineering. *The FEBS journal*, 278(16), 2753 - 2766.

Page R., Grainger M., Laforest Martin. (2018). Target and Non–target site Mechanisms Confer Resistance to Glyphosate in Canadian Accessions of Conyza canadensis. *Weed Science*. 66, 234-245.

Pedersen, B. P., P. Neve, C. Andreasen, and S. B. Powles. (2007). Ecological fitness of a glyphosate resistant Lolium rigidum population: growth and seed production along a competition gradient. *Basic Appl. Ecol*. 8, 258-268

Picoli, J., Carbonari, C., Matos, A., Rodrigues, L., Velini, E. (2017). Influence of Glyphosate on Susceptible and Resistant Ryegrass Populations to Herbicide. Brazilian Weed Science Society. *Planta Daninha*, 35.

Rahman, M. (2016). Herbicidal weed control: benefits and risks. Adv. in Plants and Agric. Res., 4(5), 371-372.

Renhua, Z. Hongbo, S. Zhaoling, L. Xiamin, S. Xinzhai, T. Becker, F. (2001). The potential information in the temperature difference between shadow and sunlit surfaces and a new way of retrieving the soil moisture. *Science in China Series D: Earth Sciences.* Vol. 44(2), 112-123.

Reddy, K. Huang, Y. Lee, M. Nandula, V. Fletcher, R. Thomson, S. Zhao, F. (2014). Glyphosate-resistant and glyphosate-susceptible Palmer amaranth (Amaranthus palmeri S.Wats.): hyperspectral reflectance properties of plants and potential for classification. *Pest Manag. Sci.* 70, 1910-1917.

Sammons, R. Heering, D. Dinicola, N. Glick, H. Elmore, G. (2007). Sustainability and Stewardship of Glyphosate and Glyphosate-resistant Crops. *Weed Tech*. 21(2), 347-354

Shirzadifar, A. (2018). Identification of Weed Species and Glyphosate-Resistant Weeds Using High Resolution UAS Images. PhD diss. Fargo, ND. North Dakota State University, Department of Agriculture and Biosystems Engineering.

Shi, L., Duan Q., Ma X., Weng M. (2011). The Research of Support Vector Machine in Agricultural Data Classification. IFIP Advances in Inform. and Comm. Tech. 370, 265-269.

Soil Survey Staff. (2005). Kindred Soil Series. Natural Resources Conservation Service, United States Department of Agriculture. Official Soils Series Descriptions. Retrieved from https://soilseries.sc.egov.usda.gov/OSD_Docs/K/KINDRED.html

Soil Survey Staff. (2014). Fram Soil Series. Natural Resources Conservation Service, United States Department of Agriculture. Official Soils Series Descriptions. Retrieved from https://soilseries.sc.egov.usda.gov/OSD_Docs/F/FRAM.html

Stoll M., Jones H. (2007). Thermal Imaging as a Viable Tool for Monitoring Plant Stress. J. Int. *Sci. Vigne Vin*, 41(2), 77-84.

Thompson, L. Puntel, L. (2020). Transforming Unmanned Aerial Vehicle and Multispectral Sensor into a Practical Decision Support System for Precision Nitrogen Management in Corn. *MDPI Remote Sens.* 12, 1597.

USDA-NRCS. (2020). Amaranthus L. pigweed. PLANTS Database. Washington, D.C.: USDA-NRCS. Retrieved from https://plants.usda.gov/core/profile?symbol=AMARA

Veysi, S.; Naseri, A.; Hamzeh, S.; Bartholomeus, H. (2017). A satellite based crop water stress index for irrigation scheduling in sugarcane fields. *Agric. Water Manag*. 189, 70–86.

Xu, R. Changying L. Paterson, A. (2019). Multispectral imaging and unmanned aerial systems for cotton plant phenotyping. *PLOS ONE. https://doi.org/10.1371/journal.pone.0205083*

Xu, S., Hossain, M.M., Lau, B.B., To, T.Q., Rawal, A., Aldous, L. (2017). Total quantification and extraction of shikimic acid from star anise (llicium verum) using solid-state NMR and cellulose-dissolving aqueous hydroxide solutions. *Sustainable Chemistry and Pharmacy*, 5, 115-121.